Chapter 2
Overview of Thermal Spray

Abbreviations

ALR	Mass ratio between gas and suspension
CFD	Computational fluid dynamics
d.c.	direct current
D-gun	Detonation gun
HVOF	High-velocity oxy-fuel flame
PACVD	Plasma-assisted chemical vapor deposition
PECVD	Plasma-enhanced chemical vapor deposition
PSZ	Partially stabilized zirconia
PTA	Plasma-transferred arc
PVD	Physical vapor deposition
r.f.	Radio frequency
RGS	Gas to liquid volume flow rates (generally over 100)
slm	Standard liter per minute
TBC	Thermal barrier coating

2.1 Surface Treatments or Coatings

2.1.1 Why Surface Treatment or Coatings

In order to be competitive in the market, it is important to be able to produce surfaces that wear only a little, are more resistant to tarnishing and corrosion, and retain their electrical, optical, or thermal properties over a long period. It is also interesting to have technologies to simplify product ranges or maintenance requirements. Surface treatments and coatings have a prominent role to play in this respect [1].

P.L. Fauchais et al., *Thermal Spray Fundamentals: From Powder to Part*,
DOI 10.1007/978-0-387-68991-3_2,

2.1.2 Surface Treatments

For surface treatments many solutions exist [1–3] and only the most important ones will be cited.

2.1.2.1 Strain Hardening

In strain hardening, materials are submitted to plastic deformation processes either prior to the application by rolling and impact loading, peening (shot or water jet), or are strain hardened in service (when using materials with a high rate of strain hardening such as austenitic manganese, stainless steel,. . .). The depth of hardening is below 1 mm for rolling but it can reach a depth as high as 20 mm for impact loading and it is around 0.5 mm with shot peening while with a water jet it is below 0.1 mm.

2.1.2.2 Surface Hardening

In surface hardening by thermal treatment, hardenable grades of steels are heated to the austenitizing temperature and cooled faster than the critical cooling rate of the steel. This can be achieved by heating with flame, induction, high-frequency resistance, plasma, laser, and electron beam. The depth of hardening is between 0.5 and 5 mm.

2.1.2.3 Thermo Chemical Treatments

In thermo chemical treatments: chemical elements are introduced by diffusion into surfaces at elevated temperatures (around 930 °C for carburizing low-carbon steel and 500–540 °C for nitriding). The elements are mainly not only carbon and nitrogen but also niobium and vanadium, which are diffused into steels to form, for example, very hard carbon layers. The different treatments comprise carburizing, carbonitriding, nitriding, nitrocarburizing, and boriding. In the normal carburizing cycle the depth of the carburized area is $x(\text{mm}) = 0.635\sqrt{t}$, where t is the treatment time in hours. Shorter times are obtained with gas (CO, CH_4. . .) carburizing: 4 h for a depth of 1–1.25 mm and this treatment time can be reduced with plasmas.

2.1.3 Coatings

If in surface treatment the process must be adapted to the part material, coatings allow depositing at the part surface various materials, which are quite different from that of the part, and almost independent of it [1–3]. They are generally categorized into thin (roughly below a few micrometers) and thick coatings (about over 50 μm), with of course intermediate thicknesses. It is generally admitted that four different techniques can be used to deposit coatings.

2.1.3.1 Electro/Electroless Plating

Electrochemical treatments [4]: In electroplating a coating is electrodeposited upon an electrode (the part to be coated), which is generally the cathode. Metals and alloys are deposited that way, except aluminum and titanium. In brush plating, handheld plating tool is used instead of a bath. For anodizing aluminum and its alloys, where an oxide layer is developed at their surface, the materials are the anodes in an aqueous electrolytic solution.

Chemical treatments [5]: In electroless plating the deposited material is reduced from its ionic state in solution by means of a chemical reducing agent, instead of the electric current. In phosphating, a metal surface reacts with an aqueous solution of a heavy metal salt, primarily phosphate, plus free phosphoric acid, to produce an adherent layer of insoluble complex phosphates,

Hot dip coatings [6]: the parts to be coated are dipped into a molten bath of coating material. Metals used, generally to protect steels from corrosion, are low-melting temperature ones such as zinc, zinc alloys, aluminum, aluminum alloys, and lead–tin alloys. The zinc is the most used material in an operation called galvanizing.

Metal coatings obtained with these techniques have thicknesses between about 10 μm and 1 mm. Their advantages are that they are omnidirectional (all surfaces exposed to the liquid are coated, including blind holes where the liquid can penetrate) the substrate is kept at a relatively low temperature and their cost (equipment and operating) is low.

2.1.3.2 Chemical Vapor Deposition

Coatings are obtained from the gaseous or vapor state [7, 8]. The coating results from the decomposition of chlorides, fluorides, bromides, iodides, hydrocarbons, phosphorus, and ammonia complexes. The gaseous precursor is thermally decomposed to produce the coating on the component surface, which is at high temperature (800–1,100 °C), thus limiting the choice of the substrate material. When exothermic chemical reactions occur at temperatures lower than the decomposition temperature the substrate surface temperature is correspondingly lowered.

The process, working at pressures between 13 and 100 kPa, is omnidirectional and gaseous mixture can easily penetrate into blind holes and deposit the coating, even on the internal surfaces of porous bodies. When using organometallic precursors the part temperature is lowered (400–600 °C) and the pressure range varies from 0.13 and 10^5 Pa.

With Chemical vapor deposition (CVD), metals, alloys, intermetallic, boron silicon, borides, silicides, carbides, oxides, and sulfides are deposited. The control of the coating microstructure depends on the temperature and the super saturation (ratio of the local effective concentration of the deposited material to its equilibrium concentration). With the high temperature of the substrate, diffusion between coating and substrate occurs easily resulting in a good diffusion bonding.

To coat small components (3 μm to 3 mm) fluidized beds are used. The bulk density of the bed can be varied between 1,800 and 19,000 kg/m^3 and it can be easily adjusted to that of the parts to be treated, and the reactive gases circulate in the bed kept in a furnace at the right temperature for the CVD reaction to occur.

To work at lower temperatures (25–400 °C), the decomposition of the precursor is achieved with plasma (Plasma-enhanced chemical vapor deposition: PECVD or Plasma-assisted chemical vapor deposition: PACVD) [9, 10]. It allows using all types of substrates including polymers and the deposition rates are higher than those of thermal CVD. The energy necessary for the activation of the gas is supplied by means of plasmas produced by either glow discharges (d.c. voltage, pulsed d.c. voltage, radio frequency) or microwaves. For example, it is possible to achieve hard coatings of amorphous carbon (DLC: diamond-like coatings) at temperatures below 200 °C with pulsed or RF discharges where acetylene is introduced. Unfortunately the pressure is in the range 0.13 Pa and 13 kPa, thus reducing drastically the deposition rate and restricting the use to thin films (below 50 μm). Moreover the process becomes monodirectional. This process allows achieving coatings with rather complex architectures.

Even if it is possible to achieve rather thick coatings, usually CVD coating thicknesses are below 50 μm.

2.1.3.3 Physical Vapor Deposition

Physical vapor deposition includes evaporation, sputtering, and ion plating. Virtually any solid material (except certain polymers) can be deposited onto any solid material. It is a line of sight method, the processes being operated at rather low pressures (1.3×10^{-6} to 13 Pa), which implies depositing thin coatings (typically below 1 μm) with a rather low-deposition rate [11, 12].

The process comprises:

– *Evaporation*, where vapors, produced by heating a solid by different means (direct resistance, only for metals, laser, electron beam, for metals and ceramics, arc discharge, for metals,...) are condensing onto the substrate surface after almost collision less line of sight transport. Mainly metals or alloys are

evaporated but reactive gases in surrounding atmosphere allow production of carbides, nitrides, or oxides. The coating formed on a plane surface has an inhomogeneous thickness because the fraction of the total mass deposited depends on radius and angles locating the surface (cosine law). To achieve homogeneous thickness several sources must be used or the substrate subjected to an oscillatory movement. The kinetic energy of particles impacting the substrate and then the coating is low (0.1–0.5 eV) resulting in relatively poor coating adhesion. These coatings are mainly used for their optical properties and for decoration

– *Sputtering* (at pressures between 0.13 and 13 Pa), where the energy of particles ejected from the target and impacting the substrate can reach hundreds of eV (up to 1,000 eV) creating adherent and dense coatings. Sputtering with plasma is achieved with excited molecules or atoms or ions. With the diode process, ions of a heavy inert gas (argon), impact (with energies up to 1,000 eV) onto the negatively biased target from which they eject material atoms. The sputtered material flux deposits onto the substrate, which is connected or not to the positive terminal. Nonconductive materials such as refractory carbides, nitrides, and oxides cannot be deposited by sputtering while using the direct current (d.c.) glow discharge mode. Reactive d.c. sputtering or radio frequency (r.f.) sputtering must be used for these nonconductive coatings. The densities of sputtered deposits are dependent on substrate temperature and deposition rate. The deposition rate is rather low. The introduction of a magnetic field under the target intensifies the sputtering by increasing the electrons density and thus that of ions in the area where the magnetic field is parallel to the target surface: magnetron sputtering. Reactive PVD can also be used where the metal target is sputtered and then the resulting particles react with the corresponding gas to form the ceramic (for example, Al particles sputtered react with oxygen). To improve the reaction, a RF coil is disposed close to the reactive gases injection close to the substrate. However collision frequencies must be increased to promote reactions and for that the chamber pressure must be increased (0.1–1 Pa). To increase the deposition rate, arcs are used. An interruption arc, a laser flash or a high-voltage flashover arc initiates cathodic Arc PVD between the cathode (the material to be evaporated) and an anode (the chamber wall in many cases). A stream of electrons (a few tens to hundreds A) is generated and flows through the cathode, melting locally at numerous cathodic spots on the cathode surface. Cathodic Arc PVD is used for the evaporation of metals (Ti, Al, Cr, . . . and their alloys) but also carbon for hard DLC coatings. The addition of reactive gases permits deposition of nitrides, carbides,. . . This technique is more and more used in industry to coat all types of tools, for car and engine components, for hydraulic components, for medical tools and instruments, for turbine blades, in decorative coatings,. . .
– *Ion plating* equipment consists of an ion source with the extraction and acceleration system for the ions. Ions are extracted from the plasma by extractor grids while suppressor grids prevent electrons escape. The ions extracted from the plasma source drift through a field free space to reach the substrate. The flux of

high-energy particles causes changes in the interfacial region or film properties, compared to the non-bombarded deposition. The working pressure is around 1 Pa, the surrounding atmosphere being generally argon, and a negative potential of 2–5 kV is applied to the work piece that becomes the cathode of a glow discharge formed between it and the grounded parts of the setup. Argon ion bombardment initially cleans the surface and continues, while the coating material is evaporated into the plasma and deposited onto the substrate. Compared to sputtering this continuing bombardment increases nucleation and improves adhesion. PVD coating thickness is usually below 5 μm.

2.1.3.4 Pulsed Laser Deposition

Pulsed Laser Deposition (PLD) [13] uses a high-power laser beam (mostly an excimer laser $200 < \lambda < 400$ nm) focused periodically onto a target material with laser pulses of a few tens of ns and frequencies of a few tens of Hz. Locally the target material is heated by the absorbed laser energy; it evaporates or sublimed, and if the laser flux is sufficient, the gas is transformed into a dense plasma inside the plume of the evaporated material. Resulting atoms, electrons, and ions are driven away from the target at high speeds into the vacuum of controlled conditions and strike the surface of the substrate leading to the nucleation and growth of thin films with the same chemical composition as the evaporated material. Additionally, gases can be introduced inside the reaction chamber to react with the atoms or molecules from the plume and modify the chemical composition of the material deposited on the substrate surface. As already pointed out for PVD the increase of the deposition pressure confines the plume expansion allowing a homogeneous deposition over several cm^2 of substrate surface. Of course it is a line of sight process with the cone angle of about 10° above the laser impact point. Thus the process is not well adapted for large surfaces and it is limited to electronics or optic applications with thicknesses below a few μm.

2.1.3.5 Thermal Spray

Thermal spray is a generic term [1, 2, 14, 15] for a group of coating processes where the coating is deposited on *a prepared substrate* by applying *a stream of particles*, *metallic or nonmetallic*, *which flatten more or less forming platelets, called splats, with several layers of these splats forming the coating*. Upon impact a bond forms with the surface, with subsequent particles causing a build-up of the coating to its final thickness. Figure 2.1 illustrates the principle of the plasma spray process. Alternate spray processes use either axial or radial powder injection in a high-energy flow resulting from combustion or high-velocity gas streams (cold spray). Coating thicknesses are between 50 μm and a few mm.

The process consists of generating an energetic gas flow (hot or cold gases) with an appropriate torch or gun (described in detail later on), generally flowing into the open-air environment, or sometimes into a controlled atmosphere. Thermal spray torches are devices for feeding, accelerating, heating, and directing the flow of a

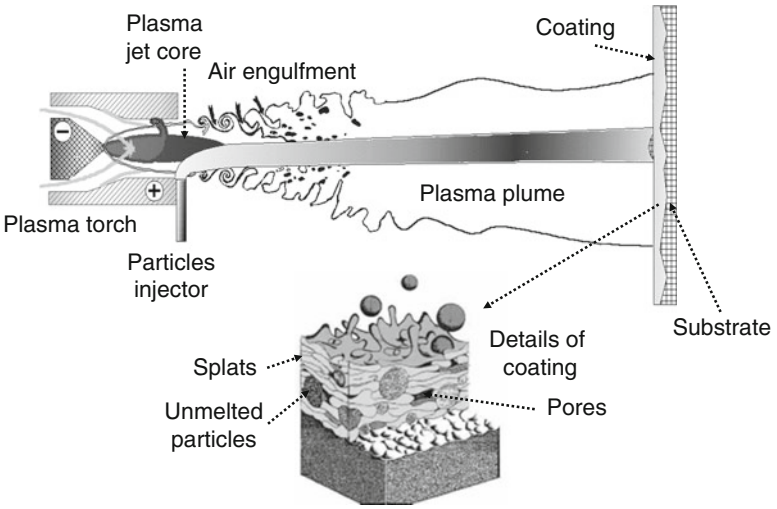

Fig. 2.1 Schematic of the different steps of the plasma spray process with radial injection of the powder in a d.c. plasma jet [16]

thermal spray material toward the substrate. The feedstock is introduced as powder, wire, rod, or cord. Wires, rods, and cords are continuously advanced (in most cases axially) at a velocity allowing the spray gun to melt their tips. The molten material is generally atomized and accelerated by an auxiliary gas fed into the spray gun, and *only molten particles are accelerated towards the substrate*. This is not the case when powders are used as the feed material. The powders are introduced into the jet of hot gases, are *accelerated but not necessarily melted before impacting on the substrate* (depending on their size and trajectories). When sprayed with a cold gas, *ductile* particles stick to the substrate and then to the previously deposited layer if their velocity is above a critical velocity, which cannot necessarily be attained by all particles of a powder with a given size distribution. As particles residence times within the spray gas, which temperature is below 600 °C, are very short (a few tens to a few hundred μs), the oxide content of coatings is almost that of sprayed particles.

Most spray processes operate in air as the surrounding atmosphere, resulting in some coating oxidation, which is drastically increasing with the temperature of the sprayed particles. This oxidation can be suppressed, or at least significantly reduced, if spraying is performed in a controlled atmosphere or a soft vacuum or achieved with the cold spray process. Moreover, for plasma-sprayed coatings of metals or alloys, a soft vacuum allows keeping the substrate at a high temperature promoting good adhesion by diffusion bonding, provided the substrate has been cleaned from its oxide layer for example by a reverse arc. However, the cost of the controlled atmosphere or soft vacuum equipment is significantly higher, almost by an order of magnitude, compared to the equipment designed for spraying in an open

Table 2.1 General characteristics of main coating methods [2]

Characteristics	Electro/electroless plating	CVD	PVD	Thermal spray
Equipment cost	Low	Moderate	Moderate to high	Moderate to high
Operating cost	Low	Low to moderate	Moderate to high	Low to high
Process environment	Aqueous solutions	Atmospheric to medium vacuum	Hard vacuum	Atmospheric to soft vacuum
Coating geometry	Omnidirectional	Omnidirectional	Line of sight	Line of sight
Coating thickness	Moderate to thick 10 μm–mm	Thin to thick 10 μm–mm	Very thin to moderate	Thick 50 μm–cm
Substrate temperature	Low	Moderate to high	Low	Low to moderate
Adherence	Moderate mechanical bond to very good chemical bond	Very good chemical bond to excellent diffusion bond	Moderate mechanical bond to good chemical bond	Good mechanical bond
Surface finish	Moderately coarse to glossy	Smooth to glossy	Smooth to high gloss	Coarse to smooth
Coating materials	Metals	Metals, ceramics, polymers	Metals, ceramics, polymers	Metals, cermets, ceramics, polymers

air environment. Besides the increased cost, the finite volume of the containment vessel limits the size of the parts that can be sprayed.

The enthalpy of the hot gas jet can be adjusted for spraying metals, alloys, cermets, or ceramics. Whatever spray process is used, it is a line-of-sight process. Thus only parts that the spray gun or torch can "see" are coated. It is for example impossible to coat small deep cavities into which the spray gun cannot fit.

Recently new processes based on the injection of a liquid into thermal spray jets have been developed [17]. The liquid is either a solution of different precursors (mixture of nitrates in water/ethanol, mixtures of nitrates, and metal-organics in isopropanol, mixed citrate/nitrate solution, etc.), or a suspension of submicron or nanometric particles. Finely structured or nanostructured coatings are obtained with thicknesses between 5 and 100 μm, bridging the gap between conventional spraying (>50 μm) and PVD (< few μm) processes. Table 2.1 from T. Bernecki [2] summarizes the different properties of the major coating methods, which are complementary and not competitive.

Thermal spray, to which this book is devoted, comprises only a small part of the total coating sales. In the next section the applications of thermal spray processes will be briefly discussed. This section is followed by a description of the different thermal spray processes and the various components of the process, i.e., preparation of the substrate, introduction of the spray material, energy transfer to the gas, interaction of the spray material with the gas, and the formation of the coating.

2.2 Brief Descriptions of Thermal Spray Applications

Choosing a thermal spray material for an application is more complex than selecting a wrought or cast material for the same applications because coating properties are not as predictable as those of conventional materials. However, now many applications are well established and new ones are continuously being developed. The optimal pairing of base material and surface coating properties is now possible and it allows obtaining a combination of characteristics that would not be possible with homogeneous materials. Aircraft and aerospace industries have provided an ideal proving ground for testing and integrating a few coating concepts. The technology has advanced to a point where it has increased the credibility and reliability of coatings. They have led to applications in other markets such as paper machines, printing, steel and metal processing, in the textile, chemical, oil, gas, automotive industries, for coatings on plastic, parts of pumps, pneumatic and hydraulic systems, near net shaped parts in rapid prototyping, and parts in the turbine, nuclear, electronic, and electrical industries. However it must be kept in mind that different spray techniques exist which are complementary and not competitive in the majority of cases, i.e., most of the time an optimal spray technique exists for a specific application. The most common functions of thermal sprayed coatings are [2, 14, 15]:

- *Wear-resistant coatings* against abrasion, erosion, cavitation wear, galling, fretting, friction, etc., and often more than one aspect of wear can be addressed. For example, cermets combine hardness, ductility, and acceptable thermal conductivity. Nonstick materials with low-friction coefficients can be combined with hard coatings. Self-lubricating materials can be deposited (for example, materials containing free carbon, or MoS_2). Very hard materials can be obtained with ceramics, which can also be combined (for example, ZrO_2 and Al_2O_3). Corrosion and wear-resistant materials can be combined.
- *Corrosion-resistant coatings*: many materials are used such as zinc, aluminum (which represents the broadest atmospheric protection), nickel-base alloys, copper–nickel alloys, chemically inert ceramics, plastics, and noble metals. One of the big concerns with thermally sprayed coatings used against corrosion is the interconnected porosity. To make the coatings impervious, high-energy thermal sprays are used, or sealants, of course, depending on service temperature. Coatings can achieve protections against high-temperature ($<$1,500 °C) corrosion or oxidation. Cold spraying seems to offer interesting possibilities against corrosion due to their high density, especially for Al, Zn, Zn–Al coatings.
- *Thermal insulation coatings*: thermal barrier coatings (TBCs) became a great success of thermal spray technology. They are made of stabilized or partially stabilized zirconia (a low-thermal conductivity ceramic material: $K < 1.5$ W/m.K when sprayed) sprayed on a superalloy bond coat protecting the substrate from oxidation or corrosion. It is worth to note that corrosion by hot gases decreases through the temperature drop achieved within the ceramic coating.

The latest TBCs are vertically segmented to have a better compliance to the stress generated when heating and cooling them. Much effort is also devoted to develop deposition processes for nanostructured TBCs, and new materials, for example, with pyrochlore structure, which has no phase transformation at high temperature as zirconia does.

- *Abradable and abrasive coatings*: these coatings are used in gas turbine engines for clearance control. Blade tips are designed or coated to make grooves in the relatively soft abradable coating face. The coating thus creates a gas-path seal that prevents gases from bypassing the blades, increasing the engine performance. Nickel/graphite, nickel/bentonite, nickel/polyester, and aluminum/polyester are used or more generally a metal matrix with a nonmetallic filler (graphite, polyester, polyimide, boron nitride, or a friable mineral). The abrasive coatings made of oxides or carbides which can also be imbedded in a metallic matrix are applied to the blade tip to reduce wear as it rubs against the abradable coating.
- *Electrically conductive coatings*: electrical contacts are made of silver, copper, aluminum, tin alloys, and bronze alloys. Thus electrical conductivity depends on the spray technique used and is generally between 40 and 90 % of that of the bulk material.
- *Electromagnetic shielding* can reduce electromagnetic or radio frequency interference, which can damage electronic components or disturb low-level signals. Such shielding is, for example, achieved by a metallic coating, often wire arc sprayed, on the inside surface of an instrumentation cabinet which is usually made of plastic or a composite material. In another application, conductive material coatings are cold sprayed on aluminum surfaces. Microwave integrated circuits (MIC) are made by plasma-sprayed Mg–Mn ferrite. Al, Ta, and Nb capacitor electrodes are sprayed in air. Unusual conductors such as aluminum titanate, barium titanate, molybdenum di-silicide, and other ceramic compounds are also sprayed.
- *Electrically resistive or insulating coatings*: electrically insulating surfaces (mostly oxides and especially alumina) are used for dielectrics (for example, in ozonizers), high-temperature strain gages, oxygen sensors (ionic conduction of zirconia), and insulation of heating coils. Resistors are made of NiCr or super alloys doped with alumina particles to tailor their electrical conductivity.
- *Electrochemical active coatings* including solid oxide fuel cells (SOFCs) and high-temperature electrolyser (HTE) are very efficient devices that electrochemically convert fuel energy into electricity and heat (SOFC) or electricity into hydrogen (HTE). SOFCs are well suited as cogeneration units for providing electricity and heat to buildings. They could greatly reduce the consumption of fuels, lowering greenhouse gas and pollutant emissions, but their development is hindered by high cost of manufacturing through wet-ceramic techniques (tape casting and screen printing). The HTE, working according to the reverse reaction of SOFC, produce hydrogen from water vapor. Plasma spray processes instead

of wet-ceramic techniques could significantly reduce manufacturing costs and many works, with industrial applications, have been devoted to these techniques.
- *Heat transfer improvement* is achieved with high-thermal conductivity coatings such as Cu or Al, or BeO for ceramics when electrical insulation is mandatory.
- *Medical coatings* can be bioactive or biocompatible or bioinert. Bioactive coatings are made of hydroxyapatite, or tricalcium phosphate, that emulates the characteristics of bone material and induces the growth of new bone attached to the implant. Biocompatible materials are made of titanium alloys, mainly Ti-6Al-4V, and Ti-6Al-7Nb, Ti-13Nb-13Zr,. . . as well as TiO_2. Titanium alloys have big pores at their surface allowing the growth of new tissue to secure the implant. SiO_2–CaO–P_2O_5-based bioactive glasses and glass ceramics are attractive materials for biomedical applications, because of the excellent levels of bioactivity. The main applications are dental, hip, and knee implants.
- *Dimensional restoration coatings* are used for salvage of worn or over-machined parts. All spray processes are used for this salvage work and very often NiCr and NiAl materials are used. With plasma-transferred arc processes coating thicknesses can reach a few mm. Cold spray has been successfully used to impart surface protection and restore dimensional tolerances to magnesium alloy components.
- *Free-standing shapes*: parts are fabricated from hard-to-machine materials by building a coating on a removal form. This process is often less costly than conventional processing methods such as sintering or hot isostatic pressing. Ceramic membranes, ceramic tubes (1 m in diameter, 10 m long, and with wall thickness of a few mm), rocket nozzles, and ceramic or refractory material crucibles are manufactured this way.
- Nuclear applications: in addition to the usual mechanical applications (however with short lifetime elements: no cobalt, for example) thermally sprayed coatings are used in Tokomak reactors and magnetic fusion devices.
- *Polymer coatings* are used as protection against chemical attack, corrosion, or abrasion. Unlike inorganic coatings polymer coatings may have equal or better properties than their cast or molded counterpart.

To conclude, this list is far from being exhaustive but it shows the wide variety of applications of thermal spray coatings. A more detailed discussion of thermal spray applications is given in Chap. 18.

2.3 Overview of Thermal Spray Processes

The thermal spray processes can be categorized in three basic groups according to the method of energy generation.

2.3.1 Compressed Gas Expansion

Commonly known as cold spray or cold gas dynamic spraying (CGDS) makes use of a converging–diverging nozzle for the creation of a high-velocity gas stream which is used for the acceleration of the powder particles in the spraying process. In this case only cold ductile metallic or alloyed particles are sprayed, with of course no oxidation during the process. For details see Chap. 6.

2.3.2 Combustion Spraying

For the definitions see Chaps. 3 and 5 for details about processes. Three types of combustion spray guns are used:

- *Flame Spray* torches that work at atmospheric pressure using mostly oxyacetylene mixtures achieving combustion temperatures up to about 3,000 K. Sprayed materials are introduced axially. Flame velocities below 100 m/s characterize this process, and powders or wires, rods, or cords are used.
- *High-Velocity Oxy-fuel Flame (HVOF).* The combustion of a hydrocarbon molecule (C_xH_y) is achieved with an oxidizer, which is either oxygen or air in a chamber at pressures between 0.24 and 0.82 MPa, or slightly more for high-power guns fed with kerosene. A convergent–divergent Laval nozzle follows the chamber achieving very high gas velocities (up to 2,000 m/s). Mostly powders are used, which are injected either axially or radially or both, depending on the gun design. Recently liquid injection (suspensions or solutions) has been developed, mainly for axial injection. Few guns have been designed to use wires or cored wires.
- *Detonation gun or D-gun*. The detonation is mainly generated using acetylene or hydrogen–oxygen mixtures (with some nitrogen to modify the detonation parameters) contained in a tube closed at one end. The shock wave created by the combustion of the highly compressed explosive medium results in a high-pressure wave (about 2 MPa) pushing the particles, which are heated by the combustion gases. Gas velocities of more than 2,000 m/s are achieved. Contrary to the two previous devices where combustible gases and powders are continuously fed into the gun, combustible gases and the powders are fed in the D-gun in cycles repeated at a frequency of 3–100 Hz.

2.3.3 Electrical Discharge Plasma Spraying

This is achieved using arcs or plasmas with four different types of torches:

Direct Current (d.c.) plasma torches generate a plasma jet from a continuously flowing gas heated by an electric arc inside a nozzle (for details see Chap. 7). They

work with Ar, Ar–H_2, Ar–He, Ar–He–H_2, N_2, and N_2–H_2 mixtures resulting in temperatures above 8,000 K (up to 14,000 K) and subsonic velocities between 500 and 2,800 m/s. When operated under atmospheric pressure, the process is commonly known as Atmospheric Plasma Spraying (APS), while under soft vacuum conditions, it is commonly referred to as Vacuum Plasma Spraying (VPS). In a few cases supersonic plasma jets could be generated using such torches when the design of the anode nozzle is adapted. Most of the applications use powders but more recently has been used solution and suspensions precursors

Radio Frequency (R.F.) inductively coupled plasma torches in which the plasma is generated though the electromagnetic coupling of the energy into the discharge cavity. It is an electroless plasma torch that can be used for the generation of plasmas of a wide range of gases including inert, reducing, or oxidizing gas mixtures such as Ar, Ar/H_2, Ar/H_2/He, Ar/O_2, Air, etc. The plasma generated is generally of a large volume, low-energy density, and low velocity (in the 10 to 100 m/s). The plasma bulk temperatures in typically in the range of 6,000–9,000 K. Induction plasma torches are characterized by their ability to allow for the internal axial injection of powders or suspensions in the discharge cavity. Induction plasma spraying is typically carried out under reduced pressure and commonly referred to as vacuum induction plasma spraying (VIPS) (for more details see Chap. 8).

Wire arc spraying: instead of using dedicated electrodes, the arc is struck between two continuously advancing wires, one being the cathode and the other the anode. The melted tips of the wires are fragmented into tiny droplets (a few tens of μm) by the atomizing gas blown between both wires (for details see Chap. 9). The wires are necessarily made of ductile material or of a ductile envelope filled with a nonductile material such as a ceramic powder. These are commonly known as cored wires.

Direct current (d.c.) transferred arc plasma: The principle is the same as that of the blown arc in a d.c. plasma torch with the exception that the arc is transferred between a floating electrode and the substrate, necessarily metallic, which, in most cases, becomes the anode. The transferred arc induces a local melting of the substrate and the particles, heated in the plasma column, stick to the molten pool where they are melted by the transferred arc. This process is essentially similar to a welding process (for details see Chap. 10).

Figure 1.5 summarizes the gas temperature and velocity ranges in the different spray processes. To illustrate the effect of particle impact velocities and temperatures, as well as of the surrounding atmosphere, the cross sections of a coating obtained by Scrivani et al. [18] with the same CoNiCrAlY commercial powder (Sulzer Metco Amdry 955) sprayed with three different processes are shown in Fig. 2.2a–c.

The quality of the coating obtained by either of these techniques depends to a large extent on the nature of the powder or precursor and the characteristics of the spraying device. For example, coatings made using VPS, Fig. 2.2a, is generally of a superior quality that obtained by means of HVOF, Fig. 2.2b, which in turn is better than APS Fig. 2.2c. The VPS plasma jet yields very dense and oxide-free coatings.

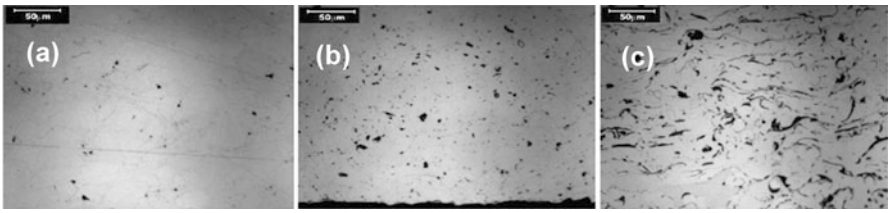

Fig. 2.2 Same CoNiCrAlY powder sprayed respectively with (**a**) the EPI system Sulzer Metco® torch working in a soft vacuum chamber, (**b**) the HVOF TAFA® JP 5000 equipment, and (**c**) the Mettech Axial III Tri-electrode Model 600 [8]

The axial plasma spray Fig. 2.2c has much better deposition efficiency than other methods, but the coating presents higher porosity, larger amounts of unmelted particles, and higher degree of oxidation. The HVOF coating in Fig. 2.2b shows low-porosity levels due to the high velocity of its flame, but the oxide content is still high compared to that of the VPS coating. Such results show that the different processes are not competitive but complementary. The choice between each of these coating techniques depends on the coating properties that are desired, the material to be sprayed, and also (probably one of the most important items) on the price the customer is ready to pay for the coating. For example, to spray a ceramic material, plasma is the most widely adopted process, as long as a high porosity coating is acceptable, flame spraying of ceramic rods is cheaper (see Chap. 18). HVOF is also possible but it requires small particles with narrow size distribution, and the deposition efficiency becomes rather low. Other spray techniques derived from the previously listed ones also exist and will be described in the corresponding chapters.

It should be noted, however, that independent of the energy source used, thermal spray processes can be divided into the following five distinct steps illustrated in Fig. 2.3.

1. *Substrate preparation* (cleaning, roughening) achieved prior to spraying and preheating. As shown in Fig. 2.4 from Yankee et al. [19] the surface preparation will define the substrate roughness characterized by its R_a, R_t, $R_{\Delta q}$,... (see Chap. 12 for definitions). Preheating the substrate above a certain temperature allows desorption of adsorbates and condensates, but this preheating also modifies the oxide layer thickness and composition with metallic substrates.
2. *Generation of the energetic gas flow*
   Expanding gas in cold spray, combustion flame or detonation, plasma or arcs, and their interaction with the surrounding atmosphere.
3. *Particle or wire or rod or cord injection*
   For powder injection, melting of particles depends on their morphology (function of their manufacturing technology, see Chap. 11), specific mass, size distribution, and trajectories that are a function of their injection parameters and the hot gases used. The choice between wires, rods, and cords depends on

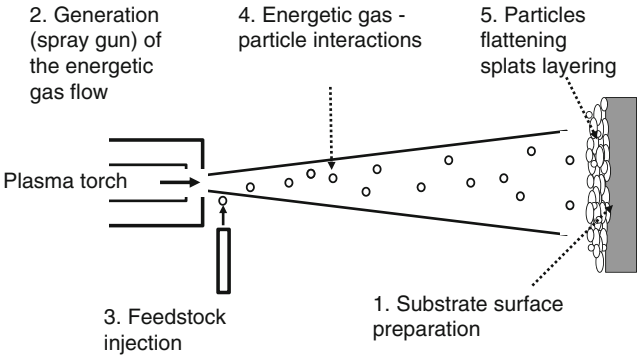

Fig. 2.3 Schematic of the different steps involved in a the thermal spray process

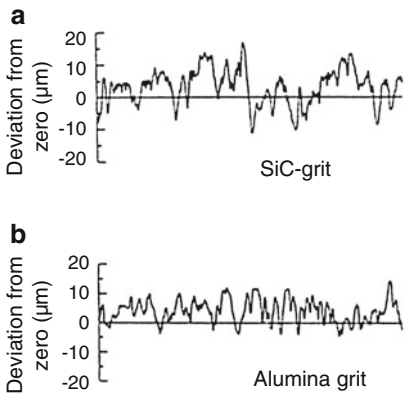

Fig. 2.4 Typical surface roughness obtained from samples roughened with (**a**) SiC and (**b**) alumina grit [19]

the material to be sprayed and the spray process chosen, and the injection velocity is controlled by the time necessary for the energetic gas to melt their tips. With this type of feeding only melted drops are sent toward the substrate.

4. *Energetic gas particle or droplet interaction*
   Involving acceleration, heating, melting, oxidation, or modification of surface chemistry of the particles or droplets (see Chap. 4). This step determines for a particle of diameter d_p, the trajectory, the impact temperature and velocity, as well as the impact angle (relative to the normal to the substrate). Depending on the entrainment of the surrounding atmosphere and the particle temperature, the particle can have its surface chemistry modified for example by oxidation (see Fig. 2.5).
5. *Coating formation*
   This depends on the particle or droplet impact, flattening, splat formation, and cooling, and splat layering first on the prepared substrate and then on already deposited layers. Particle flattening, cooling, and solidification is strongly linked, besides to its impact parameters (temperature, velocity, diameter, surface

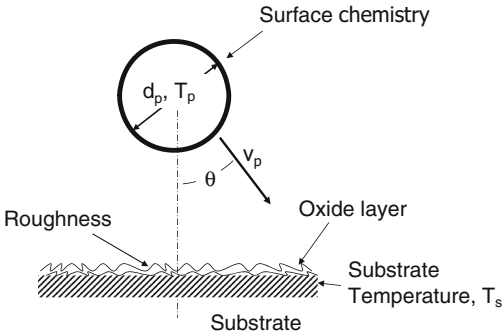

Fig. 2.5 Impacting particle and substrate parameters controlling particle flattening [20]

chemistry, and impact angle), to the substrate roughness, oxide layer thickness and composition, preheating temperature relative to the evaporation of adsorbates and condensates at its surface (for details see Chap. 13). It also depends on the relative movement between the torch and the substrate which controls the formation of beads and passes.

In the following these different steps will be described in detail.

2.4 Substrate Preparation

Substrates can be metals, ceramics, composites, glasses, woods, plastics, etc. All of these materials have very different melting or decomposition temperatures, as well as different oxidation rates generating oxide layers from thin (<50 nm) to thick (>100 nm). This means that with most spray processes, except cold spray and wire arc spraying, the substrate temperature must be controlled during spraying.

Whatever the substrate may be, its preparation prior to spraying is the most critical step for the bonding and adhesion of the coating. This preparation comprises generally three steps:

Cleaning the surface to eliminate contamination, particularly from oil or grease. Solvent rinsing or vapor degreasing are commonly used processes to remove oil, grease, and other organic compounds. For porous materials, baking is sometimes necessary. For more information see Chap. 12.

Roughening the surface (see Chap. 12 for details) to provide asperities or irregularities to enhance coating adhesion and provide a larger effective surface, as shown in Fig. 2.4. The substrate roughening in most cases is achieved by grit blasting. It is also possible to use water jets with pressures between 200 and 400 MPa. Grit blasting or water jet roughening also induces compressive stress, which can reach up to 2,000 MPa, in the first tenths of mm below the substrate-roughened surface. This stress contributes to the final stress distribution within the coating and the substrate. Some substrates (e.g., composites, plastics) require special preparations such as acid pickling.

A second cleaning step after grit blasting is necessary to remove as much as possible of the grit residues by blowing compressed air jets, using ultrasonic baths or both. Any grit particle (generally made of a ceramic material) imbedded in the substrate surface will create a defect, which is drastically magnified by an exposure to a temperature variation in most cases because of the expansion mismatch between substrate and grit materials. Of course the advantage of water roughening is that no grit residue is left. For more details see Chap. 12.

2.5 Energetic Gas Flow Generation

All devices presented below use powders or wires, rods, or cords, and introducing them into the gas flow is summarily described in Sect. 2.6, and in detail in Chaps. 4 and 11.

2.5.1 Cold Spray

2.5.1.1 Conventional High-Pressure Cold Spray

This process is "a kinetic spray process utilizing supersonic jets of a compressed gas to accelerate, at or near-room temperature, powder particles to ultra high velocities (up to 1,500 m/s). The *unmolten* particles traveling at speeds between 500 and 1,500 m/s plastically deform and consolidate on impact with their substrate to create a coating" [21].

The basis of the cold spray process [21–24] is the gas-dynamic acceleration of particles to supersonic velocities and hence high kinetic energies. This is achieved using convergent–divergent Laval nozzles. The upstream pressure is between 2 and 2.5 MPa for typical nozzle throat internal diameters in the range of 2–3 mm. Gases used are N_2, He, or their mixtures at very high flow rates (up to 5 m^3/min). For stable conditions, typically the mass flow rate of the gas must be ten times that of the entrained powder. For a powder flow rate of 6 kg/h, this means a volumetric flow rate of 336 m^3/h for helium and 52.3 m^3/h for nitrogen. Gases introduced (nitrogen or helium) are preheated up to 700–800 °C to avoid their liquefaction under expansion and increase their velocity. With the highest gas flow rate this means that the heating device must be capable of heating 90 m^3/min to temperatures up to 700–800 °C. As particles are injected upstream of the nozzle throat, the powder feeder has to be at a slightly higher pressure compared to the upstream chamber pressure. Especially when spraying with He, the spray is performed within an enclosure in order to recycle the gas.

Particles adhere to the substrate only if their impact velocity is above a critical value, depending on the sprayed material varying between about 500 and 900 m/s. The spray pattern covers an area of roughly 20–60 mm^2, and spray rates are about

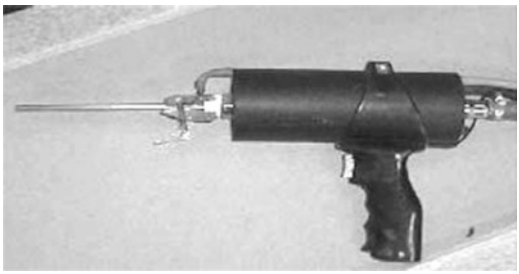

Fig. 2.6 Cold spray handgun of DYMET-402DC in 2001 [27]

3–6 kg/h. Feed stock particle sizes are typically between 1 and 50 μm and deposition efficiencies reach easily 70–90%. Only ductile metals or alloys are sprayed (Zn, Ag, Cu, Al, Ti, Nb, Mo, Ni–Cr, Cu–Al, Ni alloys, MCrAlYs, and polymers), owing to the impact-fusion coating build-up. Blends of ductile materials (>50 vol. %) with brittle metals or ceramics are also used. It is also important to emphasize that the substrate is not really heated by the gas exiting the gun (up to 200 °C at the maximum). Current and expected applications for cold spray coatings are electronic and electrical coatings (Cu, Fe–NdFeB), and coatings for the aircraft (superalloy) and automotive industries for localized corrosion protection (Al, Zn), rapid tooling repair, etc. [2]. For more details about the process see Chap. 6.

2.5.1.2 Low-Pressure Cold Spray

The cost of high-pressure spray processes is rather high, especially because of the quantity of gases consumed (especially if it is helium), and the process is not adapted at all to spraying for onsite repair of parts. Portable equipment using air has been developed [25–27] where the upstream pressure is below 1 MPa, typically 0.5 MPa with a much lower gas consumption of about 0.4 m^3/min. Figure 2.6 shows the Dymet gun developed for such a reduced pressure process.

Of course, less power (3.5 kW for the Dymet gun) is necessary to preheat the air, and the spray gas is much less expensive than N_2 or He [25]. The powder feeder can be simplified because pressurization is not necessary and the powder can be injected downstream of the nozzle throat. With gas velocities in the 300–400 m/s range the critical velocity of particles is not attained. To achieve coatings, small metal particles are mixed with bigger ones, which can be ceramics. Big particles mostly rebound upon impact, their role being to "press" the small metal particles onto the substrate and the previously deposited layers [26] (shot peening effect). Powder recuperation is hardly possible for multicomponent powder mixtures. Of course the deposition efficiency is much lower than with high-pressure guns, but the process is attractive for short production runs [27]. For more details about the process see Chap. 6.

2.5.2 *Flame Spray*

2.5.2.1 Powder Flame Spraying

This process is "a thermal spray process in which the material to be sprayed is in powder form" [28]. It is the simplest and among the oldest spray processes. The powder is fed, with a simple powder hopper or a more sophisticated powder feeder, through the central bore of a nozzle where it is heated by the oxy-fuel flame and carried by the carrier gas and the hot gas to the work piece. The flame temperature and enthalpy are determined by the fuel gas composition (C_xH_y) and flow rate and by the oxidizer (oxygen or air) flow rate [29]. For more details about the combustion process see Chap. 3. The process takes place at atmospheric pressure. One has to be reminded that one mole of air as oxidizer contains only 0.2 moles of O_2 which are used for the combustion, while the 0.8 moles of N_2 do not burn and must be heated by the flame. Thus for the same total quantity of O_2 and hydrocarbon molecules, the flame using air as oxidizer will have a lower bulk temperature.

At atmospheric pressure, the maximum temperature is achieved theoretically with the stoichiometric combustion of acetylene ($2C_2H_2 + 5O_2$) and is 3,410 K. Flame velocities depend on the combustible gas flow rates and are generally below 100 m/s. Typical flow rates are about 30 slm of O_2 and 18 slm C_2H_2 and provide a power level of about 40 kW. The specific mass of hot gas is about one-tenth of that of the cold gas at room temperature. Coatings in the "as-sprayed" condition exhibit high porosity (>10 %) and low adhesion (<30 MPa) but the coating process is easy to perform, cheap, and many materials are available. These flame spray systems are easily portable and used for many applications [30], especially to spray self-fluxing alloys, as illustrated in Fig. 2.7 for a paper machine roll coated by NiCrBSi (self-fluxing alloy). A self-fluxing alloy contains boron and silicon, which serve as fluxing agents limiting oxidation. Metallurgical bonding is achieved by heating the coating to its melting temperature after spraying. For more details about such powders see Chap. 11. The melting temperature of the substrate is necessarily higher than that of the self-fluxing alloy, and for example aluminum alloys cannot be sprayed with self-fluxing alloys and then reheated at the coating melting temperature. The process is also used for depositing wear-resistant coatings under low-load conditions, for spraying thermoplastics, rebuilding worn parts, etc., and deposition of composite coatings is possible. These coatings are used against abrasive wear (friction, erosion) and corrosion (cold or hot). For more detail about the process see Chap. 5.

2.5.2.2 Wire, Rod, or Cord Flame Spraying

This process is "a spray process in which the feed stock is in form of a wire or rod" [28] or a cord. It was the very first spray process, developed by Dr. Schoop in 1912. The setup consists of a nozzle in which acetylene is mixed with oxygen and burned

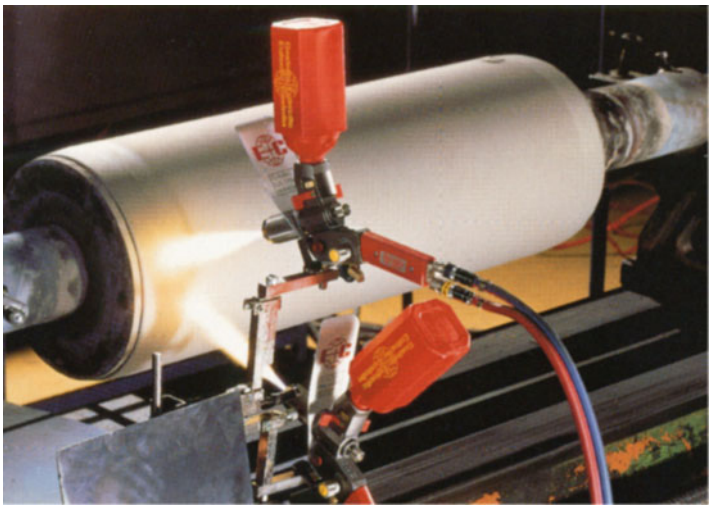

Fig. 2.7 Paper machine roll coated by NiCrBSi (self-fluxing alloy) using two powder flame guns (Courtesy of Castoline)

at the nozzle face, the flame extending into an air cap. The wire, rod, or cord is fed axially and continuously at a velocity such that the tip is melted in the flame. A stream of compressed air, surrounding the flame, atomizes and generates material droplets in a continuous stream. The advantage of the system is that only molten droplets are propelled towards the substrate. If the material is fed at a too high velocity the wire (rod or cord) comes out of the gun cap. Another advantage of the process is that the nozzle's flame is concentric with the wire or rod or cord, which maximizes the uniform heating. For example, the Master Jet of Saint Gobain can spray metal wires, cored wires, flexicords, and ceramic rods, propelled by an electromotor. The gun is lightweight and it is easy to use for spraying onto complicated shapes by hand. Of course the gun can be fixed onto a robot. For more details about the process see Chap. 6.

The remarks made previously about powder flame spraying apply to coating properties. A very wide range of materials (wires, cored wire, rods, cords) can be sprayed. All kinds of substrates can be used and the process can be manual or automated. The main applications are abrasion-resistant coatings for low-load conditions, protection against atmospheric corrosion, and copper layers for cooling. An example of a copper coating is shown in Fig. 2.8.

2.5.3 High-Velocity Oxy-fuel Spraying

This process is a "high-velocity flame-spray process" [31]. The combustion is achieved in a pressurized chamber, water-cooled or not, followed by a Laval-type nozzle (see Fig. 2.9). The combustion at pressures higher than atmospheric pressure

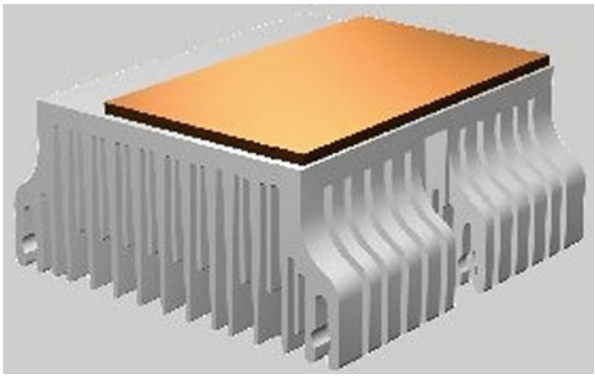

Fig. 2.8 Example of flame wire spraying: copper layer on a computer cooling system [30]

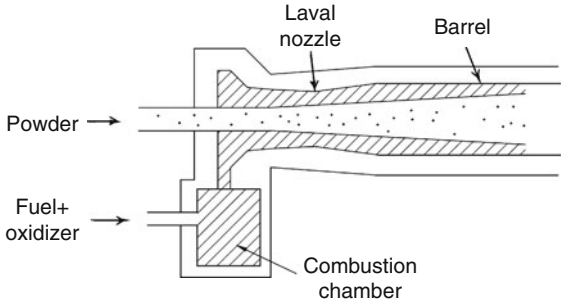

Fig. 2.9 Schematic of the HVOF process based on the Jet Kote gun [31]

(between 0.2 and 1 MPa) increases slightly the combustion temperature (see Chap. 3). For example, stoichiometric combustion of methane with oxygen at atmospheric pressure results in a temperature of 3,030 K, while at 2 MPa it is 3,733 K [29]. But the main advantage is the high gas velocity (up to 2,000 m/s, see Fig. 1.5) achieved due to the hot gas expansion through the Laval nozzle. Such velocities are supersonic as shown by shock diamonds observed downstream of the nozzle. Two types of guns exist characterized by the chamber pressure. The low-pressure HVOF uses a gun at pressures between 0.24 and 0.6 MPa with heat inputs below 600–700 MJ, while the high-pressure guns are operated in the pressure range of 0.62–0.82 MPa, generally fueled with kerosene burning either with oxygen or air with heat inputs over 1 GJ. These guns are often termed "hyper velocity guns." The "low" pressure guns are fed with hydrogen, propylene, methane, propane, heptane, and a few trademark gases together with oxygen, or also kerosene with air. The first HVOF gun was introduced in the early eighties by Browning and Witfield. Particles are injected either axially upstream of the nozzle (a pressurized powder feeder is required), as shown in Fig. 2.9 or radially downstream of the nozzle (with a conventional powder feeder). Compared to flame spraying, HVOF guns are fed with high fuel gas flow rates of 60–120 slm, and oxygen flow rates ranging from 280 to 600 slm, which corresponds to power levels of a few hundreds

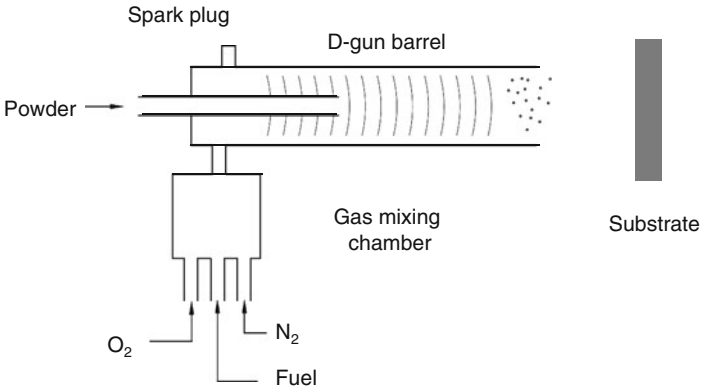

Fig. 2.10 Schematic of the D-gun [33]

of kW. With kerosene the liquid is fed between 20 and 30 slm with oxygen flows in the order of 1 m^3/min, or air up to 5 m^3/min. In flame spraying, the gas-specific mass is about one-tenth of that of the cold gas. The coupling of having highly plasticized particles impacting with high inertia allows achieving very dense coatings. The flame mixing with surrounding air can be delayed and the particles can be kept accelerating by extending the gun nozzle using a barrel (see Fig. 2.9). For the spraying of wires, special HVOF guns have been developed [32]. The principle is the same as that of wire flame spraying. The flame (propane–oxygen) is positioned at the nozzle face and the molten tip of the wire is atomized both by the pressurized flame and the airflow. Under such conditions, the gas temperature reaches values of 3,100 K, and the velocities reach values of up to 1,600 m/s, and particle velocities are much higher than with wire flame spraying.

The initial success of HVOF was in spraying dense and wear-resistant WC–Co coatings, almost as good as those sprayed by the D-gun, which at that time was only available as a service. The HVOF coatings (metals, alloys, and cermets) are dense, adherent with low-oxide content, compared to flame spraying, and they compare favorably with high-energy plasma-sprayed coatings. Typically with WC + Co (WC + NiCr or CrCo are also used) and dependent on the applications hardness values between 1,100 and 1,400 $\pm$ 150 HV_{5N} are obtained. For more details about the process see Chap. 5.

2.5.4 Detonation Gun Spraying

This process is a "thermal spray process variation in which the controlled explosion of a mixture of fuel gas, oxygen, and powdered coating material is utilized to melt and propel the material to the work piece" [28]. First developed in Russia it was introduced in the early 1950s by Gfeller and Baiker working for Union Carbide. As shown in Fig. 2.10 oxygen and acetylene are introduced in a barrel or tube (about

1 m long), closed at one end. The ignition of the mixture by a spark plug close to the closed end generates a detonation [33].

Pressures around 2 MPa are generated and particles injected about in the middle of the tube (see Fig. 2.10) are accelerated and heated, and in most cases melted. Pressures from the detonation close the gas feed valves until the chamber pressure is equalized. When this occurs the tube is flushed with nitrogen, filled with combustion gases, and the cycle is repeated (between 4 and 8 times per second or more with the recent guns). In contrast to most other spray processes the specific mass of the gas that accelerates and propels particles toward the substrate is higher than that of the cold gas (about five times) resulting in very high particle velocities. The detonation speed is the sound velocity in the combustion products (Chapman Jouget condition [29]) plus the velocity of these gases behind the wave front, as defined by Kadyrov [33]. Velocities between 1,000 and 3,000 m/s can be reached. They depend strongly on the combustible gas mixture composition and also on pressure [33]. For more details about the process see Chap. 5.

The D-Gun produces premium coatings, especially metallic and cermet ones, with properties which have been the goal of all other spraying processes to reproduce, i.e., higher density, improved corrosion barrier, higher hardness, better wear resistance, higher bonding and cohesive strength, almost no oxidation, thicker coatings, and smoother as-sprayed surfaces.

2.5.5 Direct Current Blown Arc Spraying or d.c. Plasma Spraying

This process is usually called plasma spraying. It is "a thermal spray process in which a nontransferred arc as a source of heat, ionizes a gas which melts the coating material, in-flight, and propels it to the work piece" [28]. Plasma is an electrically neutral (same amount of ions and electrons) mixture of molecules, atoms, ions (in fundamental and excited states), electrons, and photons. For gases used in plasma spraying, thermal plasma exists as soon as the gas temperature is higher than 7,000–8,000 K at atmospheric pressure (for details see Chap. 3). The plasma-forming gases: Ar, Ar–H_2, Ar–He, Ar–He–H_2, N_2, N_2–H_2 always contain a primary heavy gas (Ar or N_2) for the flow and particle entrainment and a secondary gas to improve the heat transfer (H_2, He). The high temperatures are achieved through a direct current arc struck between the cathode and the anode nozzle of the torch [34]: see Fig. 2.1. Two types of cathodes are used. Rod-type cathodes, as shown in Fig. 2.1, are usually made of thoriated tungsten, not permitting traces of oxygen or water vapor in the plasma-forming gas (tungsten oxidation starts at 1,800 K, while the cathode tip is above 3,600 K). Plasma jet temperatures are in the range of 8,000–14,000 K (at the nozzle exit on the axis). Gas flow rates are between 0.8 and 2 g/s, and it must be emphasized that the mass of the secondary gas, generally helium or hydrogen, is generally negligible compared to that of the primary gas (argon or nitrogen). Gas velocities for conventional anode nozzle internal diameters

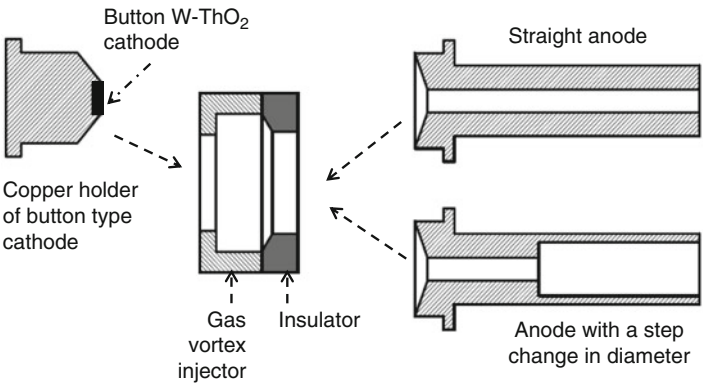

Fig. 2.11 Schematic of a d.c. plasma torch with a button-type hot cathode [35]

between 6 and 8 mm range between 500 and 2,600 m/s (subsonic velocities at these temperatures). Power levels are between 20 and 80 kW. With such temperatures the specific mass of the gas in the hottest zones of the plasma jet is about one-thirtieth to one-fortieth of that of the cold gas. Typical powder flow rates are about 3–6 kg/h. The majority of plasma spray torches make use of this type of cathode arrangement.

Button-type cathodes use a button of thoriated tungsten or other refractory metals imbedded in a copper holder, the arc being centered on it by a strong vortex flow of the plasma-forming gases. This vortex allows elongating the arc in the anode nozzle, see Fig. 2.11 [35]. Plasma-forming gas flow rates are higher (5–7 g/s) than those with a stick-type cathode, and the anode nozzle internal diameter is in 8–10 mm range. The plasma jet bulk temperature is in the 8,000–10,000 K range, with velocities below 2,000 m/s. These velocities can be supersonic at temperatures below 9,000–10,000 K. Power levels are 200–250 kW. Typical powder flow rates are up to 20 kg/h. These types of torches are used mainly for high-power/high-deposition rate applications, where the cathode attachment has high current densities. Of course other types of plasma torches exist, which are described in Chap. 7, with more detail about the plasma spray process.

The high degree of particle melting, including ceramics and the relatively high particle velocities (100–300 m/s) obtained with the plasma torches, results in higher deposit density and bond strengths compared to most flame and electric arc spray coatings [2]. To avoid any oxidation, for example, when spraying super alloys for thermal barrier bond coats, plasma spraying is performed in soft vacuum.

2.5.6 Vacuum Induction Plasma Spraying

The induction plasma spray process uses an inductively coupled r.f. plasma torch for the generation of the hot energetic gas stream in which the powder, or suspension to be sprayed, is axially injected into the center of the discharge cavity [36].

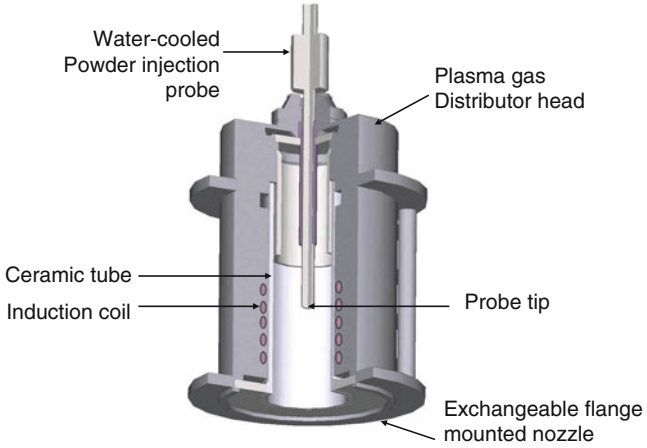

Fig. 2.12 RF induction plasma-spraying torch of Tekna (courtesy of Tekna Plasma Systems Inc., Sherbrooke, Québec Canada)

A typical design of an induction plasma torch developed by Tekna Plasma Systems Inc is shown in Fig. 2.12. The torch consists essentially of a plasma confinement ceramic tube with its outer surface cooled using a high-velocity thin-film water stream. A water-cooled induction copper coil surrounds the ceramic tube creating an alternating magnetic field in the discharge cavity. On ignition a conductive plasma load is produced within the discharge cavity, in which the energy is transferred through electromagnetic coupling. An internal gas flow introduced through the gas distributor head insures the shielding of the internal surface of the ceramic tube from the intense heat to which it is exposed. The hot plasma gases exit the torch cavity through the downstream flange-mounted nozzle. For plasma torches with r.f. power ratings between 30 up to 100 kW (mostly used in plasma spraying) and plasma gas flow rates of 50–100 slm, the bulk plasma temperature is between 8,000 K and 10,000 K, and the mean exit plasma velocity is below 100 m/s. As shown in Fig. 2.12, these torches allow for the internal axial injection of the powder or precursor, into the center of the discharge cavity using a water-cooled powder injection probe. Such torches work at pressures between 30 and 100 kPa, thus requiring a controlled atmosphere spray chamber. For more detail about the process see Chap. 8.

RF plasmas are well suited [36] for materials processing when a long dwell time of particles in the plasma is advantageous. They also offer the possibility to use reactive gases to alter or modify the particles in flight, and there is no contamination by electrode materials (no electrodes). It is a niche technology, with a big commercial success for spray powder preparation such as particle densification and spheroidization (not exclusively for spraying), as illustrated in Fig. 2.13.

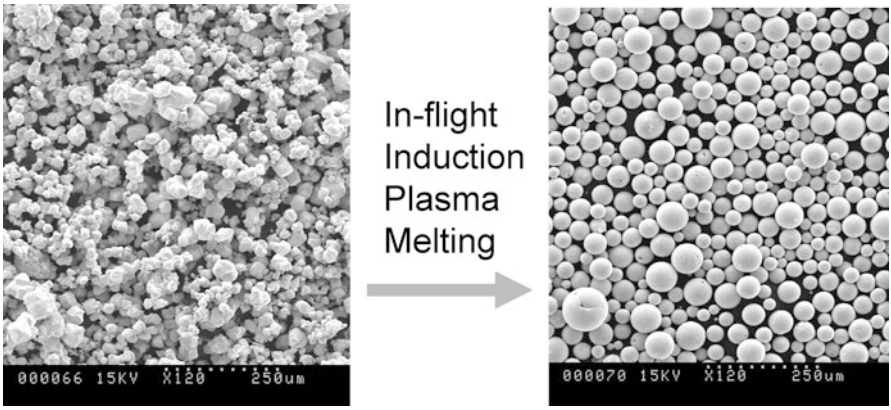

Fig. 2.13 Spheroidization of tungsten particles: initial particles diameter $d_{50} = 78$ μm, $\rho_o = 7{,}400$ kg/m3, after plasma treatment $d_{50} = 69$ μm, $\rho_o = 11{,}600$ kg/m3 (courtesy of Tekna Inc., Sherbrooke, Canada)

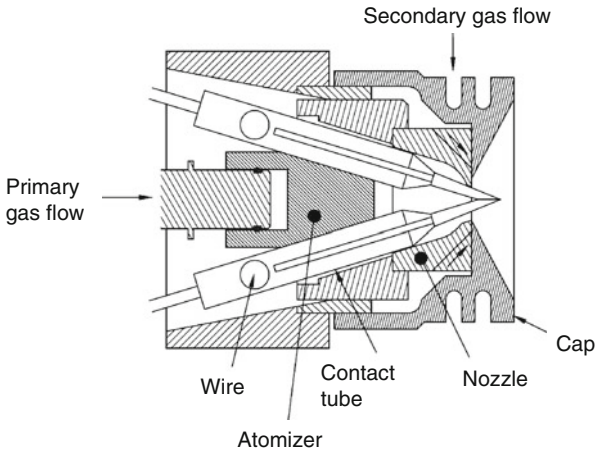

Fig. 2.14 Schematic of the wire arc spray device [37], reprinted with the kind permission of Elsevier

2.5.7 Wire Arc Spraying

This process is "a thermal spray process in which an arc is struck between two consumable electrodes of a coating material, compressed gas is used to atomize and propel the material to the substrate" [28]. In this process, shown schematically in Fig. 2.14, the two wire tips (one is the cathode and the other the anode) are continuously melted and fragmented into droplets by air jets injected with more or less sophisticated nozzles [2]. Gas velocities are a few hundreds of m/s but the gas is practically not heated by the arc, allowing one to keep the substrate temperature below a few tens of °C without cooling. Arc power levels are generally

between 2 and 10 kW, airflow ranges from 0.8 to about 3 m^3/min. The temperature within the arc can be higher than 20,000 K but the corresponding volume is relatively small. Particles are generally heated to temperatures above the melting temperature. For more details about the process see Chap. 9.

One of the main advantages of the process is the lack of substrate heating, very convenient for low-melting point substrates such as polymers. The second advantage is that the process is well suited to high-rate deposition primarily for coatings against corrosion (zinc, aluminum, zinc–aluminum) with arcs operated up to 1,500 A (with 400 A or less in conventional guns). Coatings are rather porous; contain resolidified particles and oxides (up to 25 wt%). Soft coatings can be densified by online shot peening just after deposition. Zinc is particularly efficient as cathodic protection against corrosion, especially when impregnated with epoxy paints, sealing the porosity in the coating. This process is extensively used for the protection of steel bridges.

2.5.8 Plasma-Transferred Arc Deposition

This process is "a welding process utilizing plasma. Instead of using neutral plasma, the arc is transferred to the substrate (the anode). Powder is fed into the plasma, heated, and fused to the substrate. Coatings are similar to weldments" [28]. To achieve welding the substrate (the anode) as well as the coating material must be metallic. Welding implies the formation of a molten pool on the substrate surface, which must not be blown out by the plasma flow. The plasma velocity must be low: large nozzle i.d. with a short length, low-gas flow rate, argon as plasma-forming gas with flow rates below 0.5 g/s. Figure 2.15 [38] shows a typical PTA gun. The transferred arc stability is very often improved by using an auxiliary arc between the cathode and the torch nozzle, the nozzle thus becoming an auxiliary anode at a lower potential than that of the substrate. Particles are introduced into the arc where they are heated but not melted. They stick onto the substrate where the transferred arc melts them. Depending on the gun power rather high-powder flow rates can be deposited (up to 30 kg/h). At higher power levels and higher velocities, the process allows reducing drastically the mixing of the molten materials of the substrate and the coating. It is also possible to inject two different types of powders: a metal powder close to the nozzle exit and heated below their melting temperature, and a ceramic one close to the molten bath to be included unmolten within the coating. An example of such a coating on the tooth of an excavator is presented in Fig. 2.16a, with a cross section of the coating (Fig. 2.16b) showing a good dispersion of WC irregular particles (with no evidence of melting and spheroidizing). For more details about the process see Chap. 10.

PTA deposition is generally performed on horizontal surfaces and is usually mechanized; such coatings on electrically conductive materials are often used for applications requiring repetitive operations. Compared to thermal coatings, a PTA deposit is generally more localized, denser, and metallurgically bonded to the base.

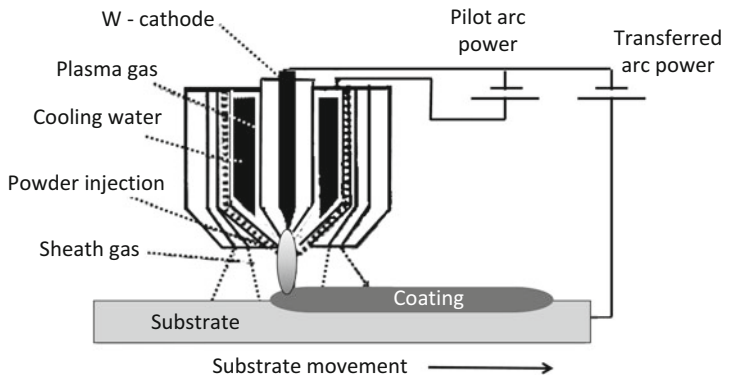

Fig. 2.15 Schematic of plasma-transferred arc (PTA) deposition [38]

Fig. 2.16 (**a**) PTA-coated tooth of excavator with Ni base coating + WC (25 kg/h) and (**b**) cross section of the coating (courtesy of Castolin)

The absence of slag removes a source of impurities. The coating is smoother and more uniform because melting takes place with a slow plasma flow and an inert gas shroud. The selection of coating materials is limited as well as the kind of substrates that can be used (for example, aluminum alloys cannot be treated by conventional PTA).

2.6 Material Injection

2.6.1 Powder Injection

Sprayed powders have sizes typically between about 10 μm and 110 μm, except for PTA where they can reach 200 μm. However, the choice of the size distribution is a key issue for the coating quality. It must be chosen according to the material sprayed, especially the difficulty of melting it, and a size distribution as narrow as possible to

limit the particle trajectory dispersion. It is important to keep in mind that the injection force of a particle is proportional to its mass, itself depending on the cube of its diameter! Particle injection is performed with an injector (in most cases a straight tube, with an internal diameter between 1.5 and 2 mm). Particles, carried by a carrier gas, collide between themselves, and the injector wall resulting in a slightly divergent particle jet at the injector exit (conical jet shape with an angle between 10 and 20°). The divergence angle increases when the particle sizes are below 20 μm and their specific mass is lower than 6,000 kg/m^3. Compared to the gas, particles have much more inertia, thus with curved injectors they will be slowed down by their friction with the curved wall, and a homogeneous distribution will be restored only 4–6 cm downstream of the bend. For more details about injection see Chap. 4.

Powders are generally characterized by their minimum and maximum diameters: for example, 22–45 μm. This means that less than 10 vol.% of the powder is below 22 μm and less than 10 vol.% is over 45 μm. However particles with the same size distribution and same chemistry can be very different. Particles can be produced through different manufacturing processes resulting in different morphologies, characterized by different densities or specific masses, various thermal conductivities, and different flow abilities (see Chap. 11). Depending on its morphology, the same particle, for a given injection velocity will have different trajectories and thus different heat and momentum transfers.

Depending on the spray gun used, powders are introduced into the energetic jet either radially or axially. Radial injection is used with d.c. plasma guns and some of the HVOF guns and sometimes in cold spray. To illustrate the radial injection, plasma spraying has been chosen, as illustrated in Fig. 2.1 from Seyed [16]. As the injected particles have divergent trajectories at the injector exit, their trajectories within the jet are also dispersed and they hit the substrate with different velocities and temperatures and of course different melting stages. For the particle penetration into the jet, it is mandatory that their mean injection force be about the same as that given to them by the energetic gas [39]. The optimum mean trajectory corresponds roughly to an angle of about 3.5–4° with the torch axis. Figure 2.17a illustrates the interaction of particles with the jet. The injection acceleration is imparted to particles by the carrier gas (see Chap. 4 where the equations for particles movement are presented in Sect. 4.2.1). The gas gives to particles of different sizes a mean velocity, which is almost independent of their size [39] and the gas velocity in the injector is also almost constant (with internal diameters of the injector below 2 mm, the Reynolds number is larger than 2,000 corresponding to turbulent flows). Thus the acceleration of particles, with a given diameter, depends only of carrier gas flow rate (see Eq. 4.4). In Fig. 2.18a the trajectory of one particle of mass m_p is optimal [39] for an acceleration γ_{p2}, where it corresponds to a trajectory making an angle of 3.5–4° with the jet axis. In contrast, the particle with the same mass but a lower acceleration γ_{p1} hardly penetrates the jet while that with a higher acceleration γ_{p3} crosses it. The major problem is, however, that particles have a size distribution with, in the best case, a value of 2 for the ratio of the larger diameter to the smaller one, corresponding to a mass ratio of 8! Thus trajectories will be necessarily dispersed as shown in Fig. 2.19 illustrating the envelope of particle trajectories

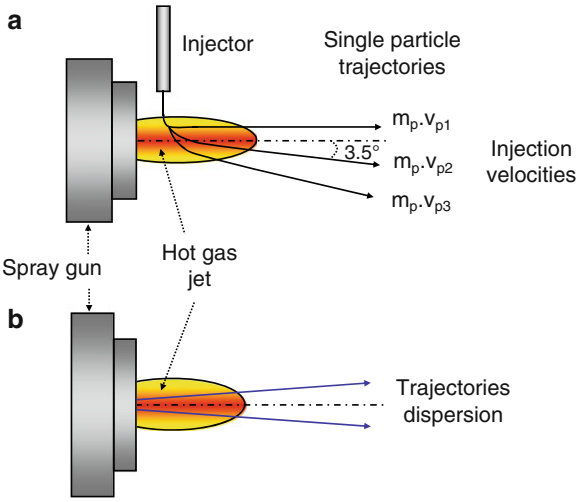

Fig. 2.17 (**a**) Trajectories of single particle injected radially with the same mass but with different injection velocities and (**b**) dispersion of particles injected axially

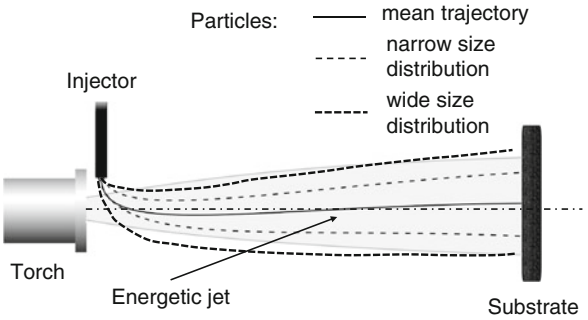

Fig. 2.18 Envelope of trajectories of particles injected radially for two powder size distributions (with one larger than the other) with the same mean size and same optimum trajectory

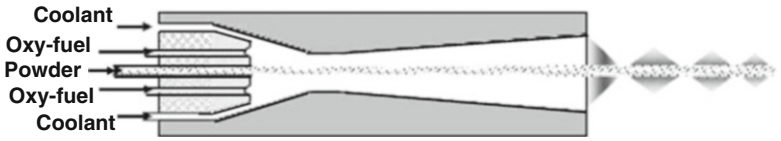

Fig. 2.19 Schematic of the axial powder injection in a HVOF gun. Reprinted with kind permission from Springer Science Business Media [40], copyright © ASM International

for two powder size distributions (with one larger than the other) with the same mean size and the same optimum trajectory. The mean trajectory is determined for the mean particle size. One can easily imagine the problem if the diameter ratio is 10 resulting in a mass ratio of 1,000!

The position of the injector relative to the nozzle exit (external or internal injection) and the torch axis plays also a key role [39]. The particle acceleration must be higher for an injection internal to the nozzle (the jet has not yet expanded).

It can be reduced with external injection, this reduction increasing with the distance from the nozzle exit due to the jet expansion. The injector must not be too close to the jet to avoid its overheating which could induce particle melting inside the injector and clogging. On the other hand, if the injector is too far away from hot gases, the injected particles bypass the plasma or flame jet.

The injection using a carrier gas is impossible for particles below 5–10 μm in diameter because the particle injection acceleration, and thus the carrier gas flow rate, would have to be increased as the square of the particle diameter. The acceleration by the carrier gas depends on the cross section of the particle (see Sect. 4.3.1) and the necessary amount of carrier gas to achieve the same acceleration of a 10 μm particle compared to a 40 μm one (16 times higher) perturbs considerably the plasma jet [39]. Moreover most powder feeders are not adapted to such small particle sizes.

Axial injection, as shown in Fig. 2.17b, is used in cold spray, flame spraying, part of HVOF spraying, certain d.c. torches such as the Mettech Axial III torch, D-gun, and RF plasma spraying. The dispersion of particles is due to on the one hand their collisions between themselves and with the injector wall and on the other to the flow turbulence. Their acceleration is much less critical than with radial injection. However when the gases flow in the spray gun is rather low, as with flame or r.f. spraying, a too high injection acceleration can perturb drastically the hot gas interaction with particles. To illustrate axial injection, the HVOF gun, shown in Fig. 2.19 from Dolatabadi et al. [40], has been chosen. As in the case of radial injection, particles at the injector exit have slightly divergent trajectories, and this divergence must be controlled to avoid that particles hit the nozzle wall, especially where the cross section is the smallest at the nozzle throat. Compared to radial injection, the particle dwell times in the hot zones of the energetic gases are longer with axial injection. The initial velocities, conferred to particles by the carrier gas are less critical than with radial injection because the gas, the flame, or the plasma flow entrains the particles, but the final particle velocities depend on their initial velocities.

Radial injection allows spraying simultaneously particles with very different properties such as ceramic and metals by using two or more injectors located at different positions. This is illustrated in Fig. 2.20 representing the injection of two different powders with two opposite injectors, thus allowing the adaptation of the carrier gas flow rates to each powder. In this figure different configurations of multi-injectors are also shown.

2.6.2 Wire, Rod, or Cord Injection

Wires, as those shown in Fig. 2.21a, are necessarily made of ductile materials. They are supplied wound on plastic spools. Their diameters are typically in the range between 1.2 and 4.76 mm. Larger, stiffer wires ($d > 2$ mm) are more difficult to feed as uncoiling requires more force and larger wire tension. Nonductile materials

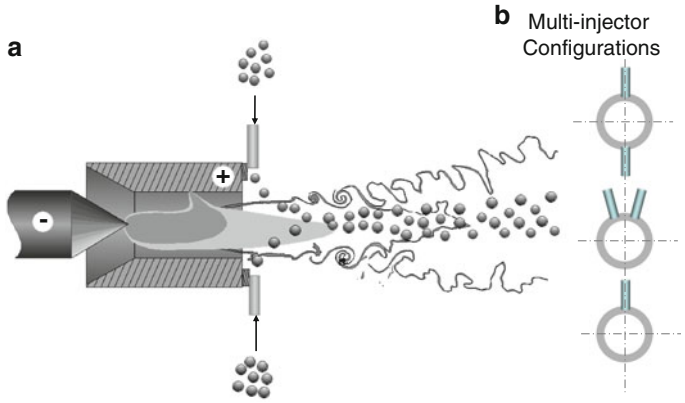

Fig. 2.20 (**a**) Injection of two different powders with opposite radial injectors and (**b**) illustration of possible configurations of radial injectors [16]

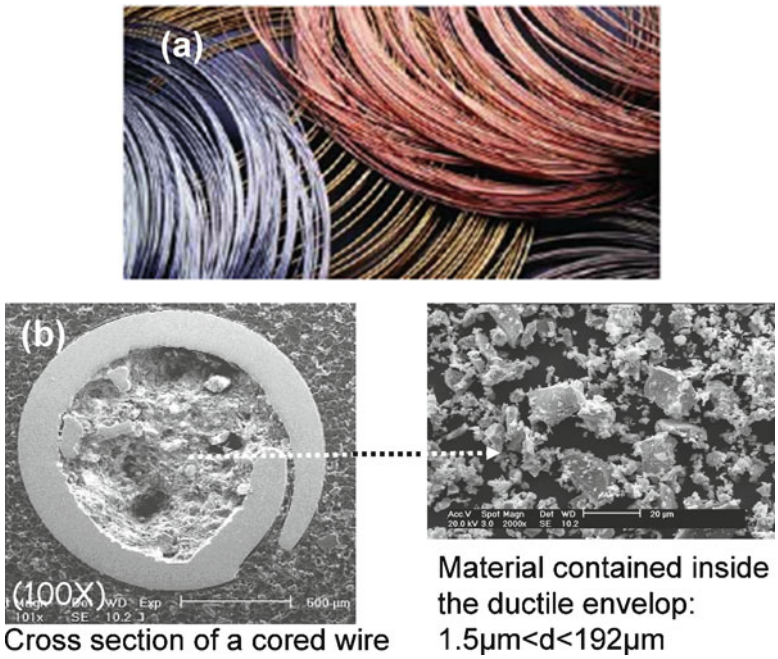

Fig. 2.21 (**a**) Different wires from Sulzer Metco (courtesy of Sulzer Metco) and (**b**) cored wire cross section

can also be used in cored wires. They consist of an outer sheath made of a ductile material surrounding one or more powdered nonductile metals or ceramics, as shown in Fig. 2.21b. Rods and cords are mainly used for ceramic materials. Rods of ceramic materials 3.16, 4.75, 6.35, or 7.94 mm in diameter have a limited length of 608 mm, which corresponds to spray times of a few minutes. Cords are made of a cellulosic or plastic casing filled with ceramic particles. The ceramic particles are within either an organic binder which starts decomposing at 250 °C and has completely disappeared at about 400 °C, or within a mineral binder such as bohemite, $Al(OH)_3$, which keeps them together up to close to their melting temperatures. Compared to rods, cords are supplied on plastic spools and their length is 120 m allowing spraying for hours. Their diameters are between 3.16 and 6.35 mm.

Wire, rod, and cords are introduced into the torch by simple mechanical devices consisting of electrical- or air-driven motors [2, 4], drive rolls, and associated speed controllers. It is of primary importance to maintain a very stable feeding rate of the material into the flame, plasma, or wire arc. The torque of the motors must be high enough to overcome the friction of the system. Drive rolls must grip the wire, rod, or cord sufficiently to prevent slipping, while not deforming the wire or crushing the rod or cord. The feeding of wires is achieved by systems, which pull only, push only, or push and pull, the latter being more complex because of the need to synchronize the two drive motors. Besides the wire guides and drive wheel geometry, critical feed issues include wire tension, wire straightness, wire diameter consistency, and wire surface characteristics.

The steady motion of the wire, rod, or cord must be adapted to the gas composition and flow rate as well as to their diameter and composition. If the wire velocity is too high, the tip cannot melt because its residence time in the flame is too short. When using low-velocity spray guns, such as a flame gun, the molten material is atomized and accelerated by an auxiliary gas fed into the spray gun. The compressed atomizing gas (generally air), fed around the flame (see Chap. 5), creates liquid metal sheets, which are disintegrating, their flapping motion is responsible for creating showers of drops. The size distribution of drops and their divergence angle depend strongly on the atomizing gas nozzle design and its flow rate. When using HVOF, instead of flame, the melted wire tip can be atomized directly by the hot gas flow.

Compared to powder feeding, the advantage of devices working with wires, rods, and cords is that *only fully melted drops are directed toward the substrate*. The way the molten wire tip form droplets has been the subject of extensive study for wire arc spraying [41]. The atomizing gas deforms the molten tips into sheets of molten metal which become self aligned in the flow, the instabilities creating droplets at their extremities (see Fig. 2.22).

For example, in the wire arc spray process, the control of the wire velocity is obtained through the control of the arc voltage, the latter depending strongly on the distance between both wires.

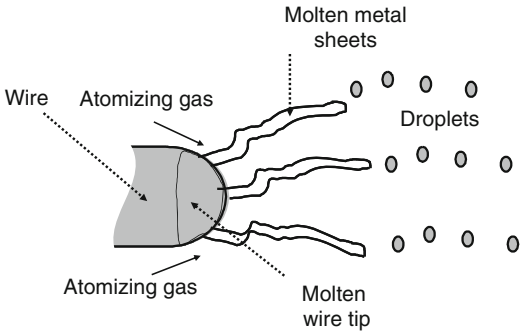

Fig. 2.22 Schematic of droplet detachment from the tip of a molten wire by the atomizing gas

2.6.3 Liquid Injection

For deposition of coatings with nanometer-sized structure, liquids (suspensions or solutions) are injected into the hot gases in the thermal spray processes. To assure sufficient energy to compensate for the cooling of the hot gases by the evaporation of the liquid and the heating of the vapor, processes where the gases have a sufficient enthalpy are used, such as HVOF or plasma spraying [17]. The liquid can be injected either by atomization with a gas or by mechanical injection (for details see Chaps. 5 and 14).

2.6.3.1 Gas Atomization

Very often coaxial atomization is used. This process consists of injecting a low-velocity liquid inside a nozzle where it is fragmented by a gas (usually Ar because of its high-specific mass) expanding within the nozzle bore [42]. The atomization is affected by the following parameters: the relative velocity liquid–gas, the ratio of the gas to liquid volume flow rates, called RGS (generally over 100), or the mass ratio between gas and suspension, called ALR (below 1), the nozzle design, and the properties of the liquid (density, surface tension, dynamic viscosity). The drawbacks of this atomization are the space, droplet diameter range (typically 5–100 μm for an air cap atomizer), divergence of the atomized droplet jet, and droplet velocity distribution (see Chaps. 4 and 14). Moreover, the atomizing gas can also perturb the hot gas flow.

2.6.3.2 Mechanical Injection

Two main techniques are possible: either to have the liquid in a pressurized reservoir from where it is forced through a nozzle of given diameter, d_i, or to add to the previous setup a magnetostrictive rod at the back side of the nozzle which superimposes pressure pulses at variable frequencies (up to a few tens of

kHz). The reservoir is connected to an injector consisting of a stainless steel tube with a laser-machined nozzle with a calibrated injection hole. The drawback of the system is that the reservoir pressure varies as the inverse of the fourth power of d_i. According to this relationship, if for a given liquid flow rate the pressure is a few tenths of MPa with a nozzle of 150 µm internal diameter, the required pressure becomes a few tens MPa if the nozzle i.d. is reduced to 50 µm (the pressure is multiplied by 81). The liquid exits the nozzle with a constant diameter jet, which is between 1.2 and 1.8 times the nozzle i.d. depending on the nozzle shape and reservoir pressure. After a distance of about 120–150 times the injector nozzle internal diameter, instabilities can be observed in the jet and a stream of uniform droplets is observed (see Sect. 4.5.1).

When using a magnetostrictive drive rod at the backside of the nozzle, giving pressure pulses with a frequency of up to 30 kHz, droplets with a constant diameter are produced, having a specific velocity. A constant distance separates these droplets.

In all these injection methods, the key issue is to control the size and the velocity of the droplets. Mechanical injection offers a controlled velocity and a constant size, although it may not be simple to achieve drop diameters below 100 µm. This control is by far more difficult with gas atomization. Besides having a distribution of droplet sizes, droplets have a more or less broad velocities distribution and the trajectories show different dispersion spray angles (see Chap. 4). Thus the injection control is sometimes tricky. For more detail about liquid injection see Chaps. 4 and 13.

2.7 Energetic Gas–Particle Interactions

2.7.1 Momentum Transfer

The particle trajectory within the high-energy jet depends on its acceleration $\frac{\partial v_p}{\partial t}$, which is linked to the force exerted on it. This acceleration is given by

$$\frac{dv_p}{dt} = \frac{18\mu_g}{\rho_p \cdot d_p^2}\left(v_g - v_p\right) \tag{2.1}$$

where μ_g and v_g are the gas viscosity and velocity respectively, ρ_p, d_p, and v_p the specific mass, diameter, and velocity of the particle.

From Eq. (2.1) it is obvious that the particle acceleration increases if the specific mass of the particle material decreases as well as its diameter, and if the gas viscosity and its velocity increases. Typical velocities of particles with their mean size range for different spray guns are summarized in Table 2.2. For more details about momentum transfer see Sect. 4.2.

According to the particle size distribution (generally Gaussian) and injection acceleration vectors, which are not all parallel to the injection axis, particles have a

Table 2.2 Typical particle size range and velocities with different spray guns

		Powder flame	Wire flame	HVOF	D-gun	d.c. plasma	r.f. plasma	Wire arc	PTA
Particle size range (μm)	Metal	10–90	Wire	<45	<45	10–90	<150	Wire	0–200
	Oxides	No	Rods–cords	<15	<15	<45	<90	No	0
Particle velocities (m/s)		<100	<200	200–700	<1,200	<350	<100	<200	20–30

rather wide distribution of trajectories within the jets and a rather broad range of velocities. It is the same with molten droplets resulting from wire, rod, or cord atomization.

2.7.2 Heat Transfer

The heat transfer mechanisms between a hot gas and a single sphere are mainly those resulting from gas convection and radiative loss of the particle to its surroundings (for details see Sect. 4.3). In the following, to simplify the presentation only the basic assumptions will be considered. For example, the heat propagation within the heated particle, depending on the value of its thermal conductivity relatively to that of the hot gases, will not be considered (for details about it, see Sect. 4.3.3). The heat from the hot gas q_{cv} (W) depends on the heat transfer coefficient h (W/m^2 K), the particle surface a (m^2), and the gas temperature T_s (K). The main energy loss of the hot particles, especially for high-temperature particles (>1,800 K), is the radiative loss to the surroundings. It is characterized by the global emission coefficient ε of the particle and the Stefan–Boltzmann radiation constant σ_S(5.671 × 10^{-8}W/m^2 K^4). Finally the most important term is the energy (J) necessary to melt the particle:

$$\int_0^{\tau} Q_{\text{int}} \cdot \mathrm{d}t > m \cdot c_p \cdot (T_m - T_0) + m \cdot L_m = Q_F \tag{2.2}$$

where τ is the residence time of the particle in the hot jet, m the mass of the particle (proportional to the cube of its diameter), c_p the specific heat (J/kg K), and L_m the latent heat of melting (J/kg). The residence time depends on the length of the hot jet and the particle velocity. These equations define the requirement for melting a particle by Q_L (J m$^{3/2}$/kg$^{1/2}$) [43]:

$$Q_L = \left(m \cdot c_p \cdot (T_m - T_0) + mL_m\right) / \sqrt{\rho_p} \tag{2.3}$$

Table 2.3 summarizes some values of Q_L for different materials. It can be seen that it is not necessarily materials with the highest melting temperature which are

Table 2.3 Values of Q_L for different materials

	T_M (°C)	c_p (J/kg K)	L_m (kJ/kg)	Q_F (kJ/kg)	$Q_L = Q_F/\sqrt{\rho_p}$
Al_2O_3	2,313	1,090	1,095	2,564	27.07
Mo	2,890	251	290	1,010	10.25
Ti	1,933	527	376	1,338	27.87
ZrO_2	2,677	566	769	2,272	30.09

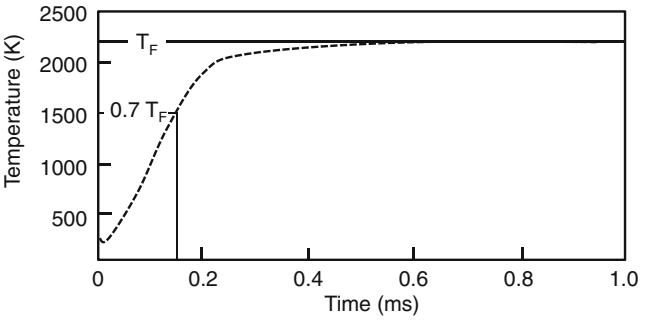

Fig. 2.23 Temperature evolution for a single particle immersed in infinite plasma at temperature T_F

the most difficult to melt, provided the gas temperature is a few hundreds of °C above the particle melting temperature.

Another important point is that when heating a single particle in an infinite medium at a uniform temperature, T_F, the particle temperature reaches that of the medium very slowly once its temperature is above about $0.7 \times T_F$ (see Fig. 2.23).

This means that when injecting a particle into a hot medium, with a limited length, particles will hardly reach 0.7 times the flame temperature. For example, with an acetylene-oxygen flame at about 3,000 K, it will be difficult to melt particles requiring heating above a value of 2,100 K. With a plasma jet at over 8,000 K, any material can be melted. Of course, this consideration does not apply when using wire, rod, or cord, the residence time of the wire tip being much longer than that of a particle (about 1 ms). Thus, it becomes possible to reach temperatures up to 0.9–0.95 times that of the flame. For a stoichiometric acetylene–oxygen flame at about 3,400 K, a zirconia rod or cord can be melted.

When the particle temperature approaches its melting temperature, particle melting and evaporation starts with the evaporation rate increasing rapidly as the boiling temperature of the material is approached. This means that it will be almost impossible to spray materials for which the melting temperature is not separated by at least 300 K from its boiling temperature (the deposition efficiency will become very low). The same considerations apply if instead of vaporizing, the material decomposes, which explains why it is generally difficult to spray most nitrides, carbides, and borides.

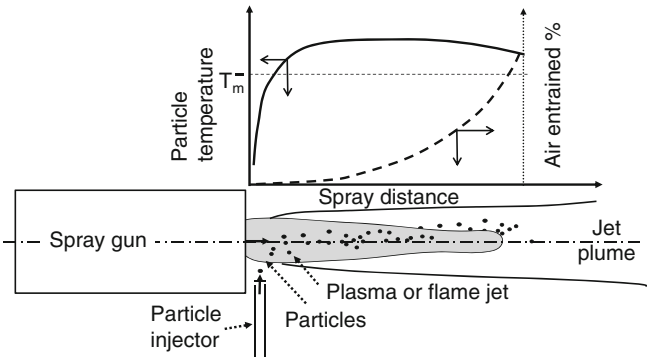

Fig. 2.24 Schematic of the air entrainment within the hot plasma jets as function of the spray distance and particle temperature evolution

Finally, due to the dispersion of their trajectories, hot particles within the jet are not uniformly distributed. The energy radiated by the hot particles can be approximated by a Gaussian distribution over the jet diameter at a specific axial location. Any variation of the spray parameters, for example, arc current or plasma-forming gas with a d.c. plasma torch, modifies the force the hot gases impart on the particles as represented by $S_p \cdot \rho \cdot v^2$; where S_p is the projected surface of the particle, ρ and v the specific mass and velocity of the high-energy plasma jet. Thus changing the carrier gas flow rate to keep an optimum mean trajectory is essential to modify the injected particle accelerations. *The key issue is that the carrier gas flow rate must be adjusted as any of the spray parameter is modified*. For more detail about particle trajectories and heat transfer see Chap. 4.

2.7.3 Effect of the Surrounding Atmosphere

Most spray processes are operated in air (atmospheric spraying). Air, or the surrounding gas if spraying is performed in a controlled atmosphere chamber, is always entrained by the high-energy jet. Thus, when spraying in air, entrained oxygen (diatomic or monoatomic in case of plasma) can react with the sprayed materials. The penetration of the entrained air in the jet increases with the distance from the nozzle exit with the expansion of the jet. For example, for a d.c. Ar–H_2 plasma jet, the entrained air penetration in the jet is limited (less than 30–40 vol.%) during the first 40–50 mm from the torch nozzle exit. Further downstream the jet becomes more and more oxidizing. At 100 mm more than 95 vol.% of the hot gas mixture is air at temperatures in the 2,500–3,500 K range (see Fig. 2.24).

2.7.3.1 Particle In-Flight Oxidation

The Arrhenius law controls the oxidation kinetics: the rate of change of concentration of a given species is proportional to the specific reaction rate constant k. The Arrhenius form of k is

$$k = A \ \exp\left(-E_A/k_B T\right) \tag{2.4}$$

where, A is a term accounting for the collision terms with mild temperature dependence, k_B is the Boltzmann constant, and E_A the activation energy of the reaction. Roughly, k increases by one order of magnitude when T increases by 100–200 K. Thus oxidation reactions will be strongly promoted when sprayed materials are heated to high temperatures. This is especially the case when the temperature is above the melting temperature where, besides the diffusion phenomenon, oxidation can be promoted by the convective movement induced within the fully melted particle by the hot gas flow around it. This situation is encountered under certain conditions in plasma, HVOF, and wire arc spraying. In that case, internal recirculation within the particle is responsible for continuously bringing fresh metal to the particle surface, while molten oxide or oxygen is entrained inside the molten particle. Compared to diffusion-controlled oxidation, the oxide content of the particle is such a case can be larger by a factor of 4 to 6!

This situation is important when the Reynolds number relative to the particle is higher than 20, and the ratio of kinematic viscosities of the gas to the liquid particle ν_g/ν_p is higher than 50 [44]. The phenomenon is particularly important when the melting temperature of the oxide is close to that of the metal, for example, in low carbon and stainless steel. The convective oxidation can result in the formation of up to 15 wt% of oxide with low-carbon steel. For more details see Sect. 4.3.3.7. To limit the oxidation of the particle, its temperature must be kept as low as possible. This is possible when increasing the particle velocity to spray it close to or below its melting temperature, as with the D-gun or high-pressure HVOF. Increasing the particle velocities also reduces their residence time within the hot gas stream where oxidation reactions occur. Of course, when using cold spray, particle temperatures are kept below a few hundred °C, suppressing or limiting the effects of high temperatures: melting, evaporation, decomposition, gas release, and oxidation.

2.7.3.2 Substrate and Successive Passes

Substrate oxidation occurs during the preheating stage before spraying; preheating performed to get rid of adsorbates and condensates. This preheating (at temperatures between 200 and 400 °C depending on the substrate material), which can also result in the partial oxidation of the substrate surface, is generally performed with the spray torch, at least when the part dimensions are not too large (less than 1 m). By controlling the preheating rate, depending on the distance and

relative torch–substrate velocity, the preheating time, and temperature, substrate oxidation can be limited. It is important to control this oxidation, especially with materials that oxidize easily, such as low-carbon steels. A thick oxide layer is generally not mechanically sound, and coatings are detaching from their substrate not because of poor coating quality, but due to the poor adhesion to the oxide layer on which they were sprayed! Once spraying has started, the substrate oxidation by the hot gases is relatively small. However, successive passes of the hot jet can increase oxidation when the coating does not consist of an oxide.

2.7.3.3 Chemical Reactions Other Than Oxidation

Chemical reactions can occur within particles in-flight and also during coating formation. Liquid–solid reactions occur within cermet particles when the ceramic particle, in the solid state, is partially dissolved in the surrounding liquid metal. One typical example is the dissolution of tungsten carbide grains (WC) in the liquid cobalt when spraying WC–Co particles. These reaction times are generally rather long (characteristic times of a few seconds) and are thus limited by the rather short flight time of the particles in the hot jets (a few milliseconds). However, these reactions, as is the case with all chemical reactions, are following Arrhenius law, and the reaction rate increases drastically with the particle superheat, for example when the cobalt matrix is above its melting temperature. This fact explains the better results that are obtained when spraying WC–Co particles with a HVOF gun (temperatures close to the Co melting point) compared to a plasma sprayed coating, where the cobalt is largely overheated.

The second type of reaction is that related to the synthesis of condensed materials by a "self-supported" heating generated by the exothermic reaction between components (SHS: self-propagation high-temperature synthesis). The reaction occurs between both materials within the particle as soon as the particle in-flight has reached the ignition temperature. Such reactions are longer than the residence time of the particle in the hot gas and they can continue after the deposition. A well-known example is the formation of NiAl when spraying particles made of a Ni core surrounded by an aluminum shell, or when spraying silicides, borides, carbides in form of agglomerated particles made for example of Ti–bronze and boron. For more details see Chap. 4.

2.7.3.4 Limiting Gas-Induced Reactions

At the end of the 1960s and at the beginning of the 1970s, inert gases have substituted air as the environment for plasma spraying. This can be achieved by spraying in a controlled atmosphere chamber either filled with a neutral gas (generally argon) or in a soft vacuum (≈10 kPa). As the process is rather costly in terms of gas consumption and equipment cost (up to one order of magnitude more than that working at atmospheric pressure in air) it is generally used only in

connection with conventional plasma spray equipment (gas flow rates below 100 slm). In controlled atmosphere spraying, the chamber walls are not necessarily cooled if the chamber volume is large enough (few m^3). The chamber air is removed with vacuum pumps and then the chamber is back filled with argon. The oxygen content is less than 7 ppm when a liquid argon source is used. Under these conditions the plasma jets are a little longer and wider than in air, because in air the dissociation of the entrained oxygen consumes a lot of energy and cools the plasma. As shown in Chapter 4, spraying in controlled atmosphere is not necessarily accompanied by an improvement of heat transfer between the plasma and the particles. The oxide content in the coatings is limited, however, to that already present in the sprayed powders.

Shroud nozzles have also been used, mostly with plasmas. The shroud nozzle is attached to the front of the plasma gun and a blanket of inert gas (argon or nitrogen) is used to displace air around the jet. Unfortunately high-inert gas flow rates are necessary (300–500 slm for conventional d.c. spray torches). Other types of shrouds supply a concentric sheath of inert gas between the hot plasma and the air. The flow rates are slightly lower. For more details see Chap. 7.

2.8 Coating Formation

2.8.1 Coatings from Fully or Partially Melted Particles in Conventional Spraying

Particles with given temperatures (above or close to their melting temperature) and velocities impact and flatten *on the prepared substrate* forming splats. The particle and substrate parameters playing a role in the particle flattening are summarized in Fig. 2.5. The critical particle parameters comprise the particle velocity and temperature at impact, the impact angle relative to the substrate (best results being obtained when the particle impacts perpendicularly to the substrate), the oxidation of the particle, and the temperature gradient within the particle (especially for low-thermal conductivity materials). Most particle flattening studies, for experimental reasons or modeling simplification, have been performed on smooth surfaces. For the substrate the key parameters are its surface roughness, as resulting from its preparation or from its oxidation (most substrates are made of metals or alloys) or both, and the substrate preheating temperature. The oxide layer thickness and composition also play an important role [20]. Modeling results of particle flattening on a smooth substrate are illustrated in Fig. 2.25 illustrating the flattening of a nickel droplets on a stainless steel substrate preheated to 563 K [45]. In experiments and models, the flattening time is in the range of a few μs, and the solidification time is longer though solidification starts before flattening is completed.

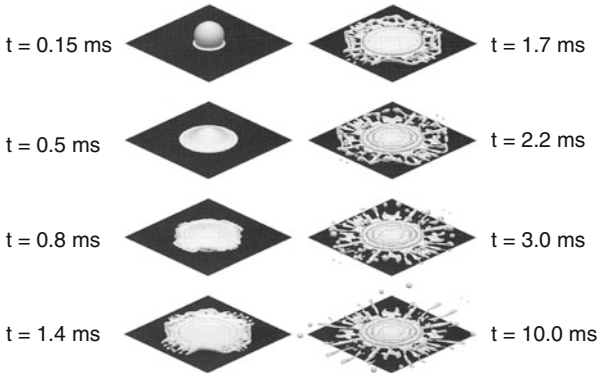

Fig. 2.25 Modeling of a nickel droplet ($d_p = 60$ µm) impacting on a smooth stainless steel substrate preheated at 563 K. Reprinted with kind permission from Springer Science Business Media [45], copyright © ASM International

As can be seen, after a relatively symmetrical flattening stage (up to 1.4 ms) digitations start to appear resulting in an extensively fingered splat. In fact, the phenomenon is very complex, depending on the dynamic wetting angles, drop surface tension and velocity, and on solidification taking place before flattening is completed and modification of the liquid flow [20]. For more details see Chaps. 4 and 13. Most experimental studies show that, for smooth substrates, above a critical preheating temperature, called transition temperature, T_t, [20, 46] splats are disk shaped, while below such a temperature they are extensively fingered. Among the different explanations the most plausible one seems to be the evaporation of adsorbates and condensates present at the substrate surface [20, 47]. Without this preheating and the evaporation of adsorbates and condensates, the local pressure under the flattening melted droplet increases rapidly resulting in the lifting of the liquid that is flowing on the substrate surface. Thus, compared to a surface where adsorbates and condensates have been eliminated, the contact surface between flattening particle and substrate is reduced by a ratio of 2 to 6 inducing the fragmentation of the liquid flow. For more details see Sect. 13.5.1.

For micrometer-sized particles, depending on their degree of superheat (above the melting temperature) and on their impact velocity (key parameter), for a substrate preheated above T_t, the ratio of the splat diameters, D, to the initial droplet diameter, d_p, is in the range $2 < D/d_p < 6$. For most sprayed materials on different substrates, the transition temperature is below $0.3T_m$ (T_m being the particle melting temperature). Thus the cooling rate of the flattening particle is practically not affected by the substrate preheating at the transition temperature. The flattening behavior of the drop above the transition temperature is mainly due to desorption of adsorbates and condensates from the substrate surface when preheated above T_t. The contact between the splat and the substrate represents up to about 60 % of the splat surface on substrates preheated above T_t, compared to possibly less than 20 % on cold substrates. Accordingly, when spraying on rough substrates preheated above T_t the coating adhesion is higher by a factor of 3 to 4 compared to that obtained on a cold substrate.

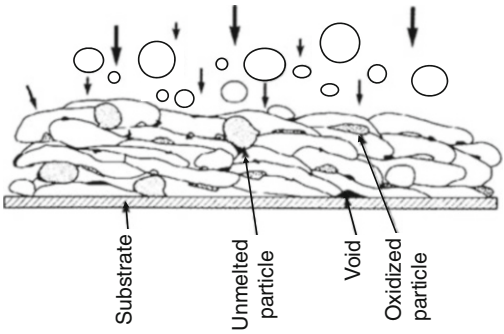

Fig. 2.26 Schematic cross section of a thermally sprayed coating

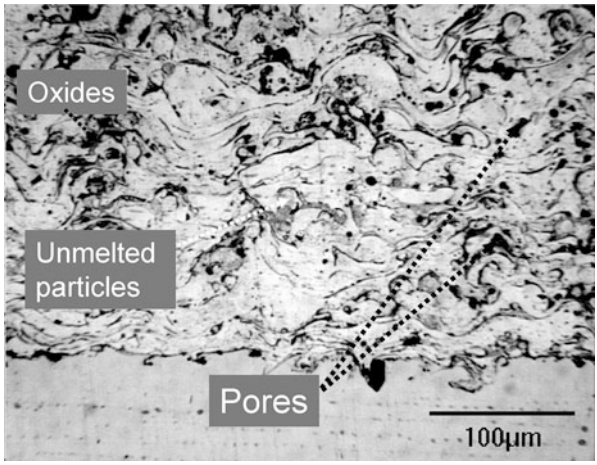

Fig. 2.27 Stainless steel coating (304L) deposited by air plasma spraying on a low-carbon (1040) steel substrate

The time between two successive impacts is typically in the range of ten to a few tens of µs. Thus the next particle impacts on an already solidified splat. The splat layering is controlled by the powder flow rate, the process deposition efficiency, and finally the spray pattern including the relative torch–substrate velocity. Coatings contain layered splats, porosities (often due to the poor ability of the flattening particle to follow the cavities present in the previously deposited layer), unmolten or partially melted particles, and oxides for metals and alloys. This is schematically illustrated in Fig. 2.26.

Coatings obtained by conventional spraying (sprayed particles with sizes of a few tens of micrometers) have thicknesses between about 50 µm and a few millimeters. Figure 2.27 presents the cross sections of a plasma-sprayed ($Ar–H_2$) stainless steel coating and Fig. 2.28 that of a plasma-sprayed yttria partially stabilized zirconia coating. Figure 2.28 shows all the coating characteristics shown in the schematic cross section in Fig. 2.26, but in Fig. 2.28 (YSZ coating) of course no oxidation is present, and the lamellar structure is more pronounced.

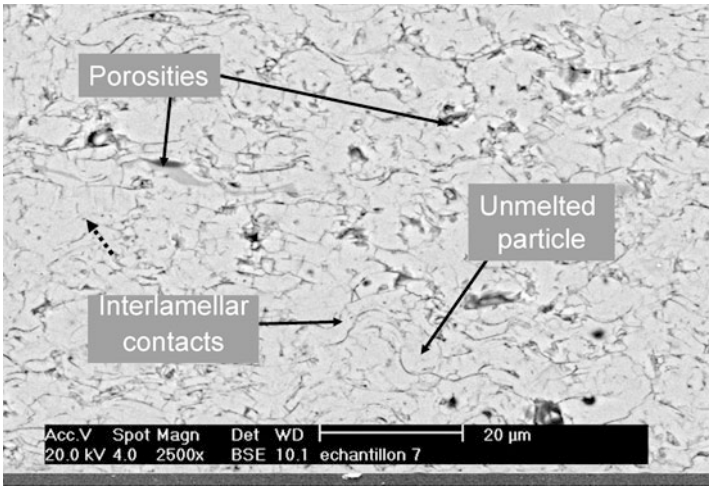

Fig. 2.28 YSZ (8 wt%) coating plasma sprayed on a super alloy

Cold-sprayed ductile particles are not melted at all at impact and they need a velocity above a critical value to form a coating. This critical velocity depends on the particle size, material, manufacturing process, and the substrate material and properties [22]. At the time when the substrate surface is placed in front of the impacting particle jet, none of the particles adhere to it and rebound. They only clean and deform the surface. After a certain "induction time" t_i, the particles begin to adhere in an avalanche-like manner, rapidly forming the coating. This induction time depends on the surface preparation [48]. The deposited particles of the first layer are little deformed and have a diameter D which is close to that of the impacting particle d_p ($D/d_p < 1.5$). For the next layers, upon impact particles are plastically deformed and the previously deposited ones are consolidated by the impact of the incoming ones. This is illustrated in Fig. 2.29.

Figure 2.29 demonstrates that such coatings can be obtained with porosities of far less than 1 %. The etching of sample cross sections reveals the internal grain boundaries of former spray particles and highly deformed grains close to particle–particle interfaces.

2.8.2 Adhesion of Conventional Coatings

2.8.2.1 Hot Particles

The bond between splats and substrate and afterwards between splat and already deposited layers is essentially mechanical. However in this case the splat diameter

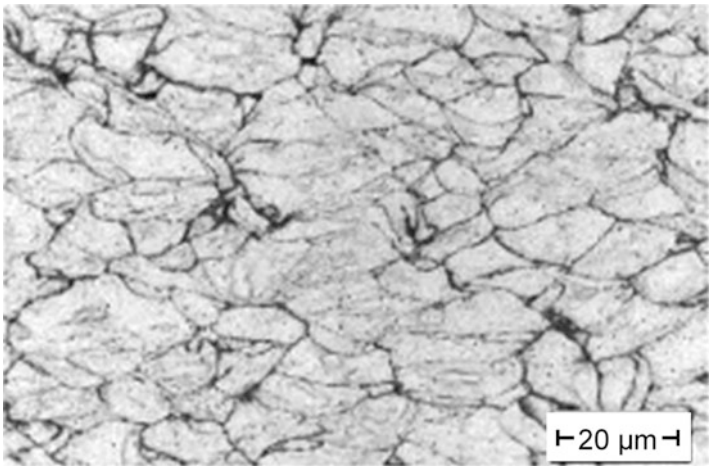

Fig. 2.29 Cu cold sprayed on Cu substrate with a trumpet-shaped standard nozzle (powder −22 + 5 µm; process gas N_2; temperature 320 °C; pressure 3 MPa): close-up view of the cross section revealing grain boundaries and particle–particle interfaces. Reprinted with kind permission from Springer Science Business Media [21], copyright © ASM International

has to be adapted to the peak heights. Roughly the splat diameter, D, must be such that

$$D = 2 - 3 \times R_t \tag{2.5}$$

where, R_t is the distance between the highest peak and deepest valley. If the splat diameter D is much smaller than R_t, the adhesion is poor. The distance between peaks is also of primary importance, because the liquid has to penetrate into the undercuts, and R_a and R_t do not account for this parameter. Thus another quantity must be considered: the root mean square value $R_{\Delta q}$ which is obtained from the local profile slope $dz(x)/dx$ of the roughness profile within the single measurement length (for details see Sect. 12.5.1). For example, for plasma-sprayed coatings on non-preheated substrates, even with the optimal roughness, the maximum coating adhesion is about 20 MPa, while with substrates preheated above the transition temperature, it is between 40 and 70 MPa. Desorption of adsorbates and condensates and sometimes the improved liquid drop–substrate wettability are responsible for the better adhesion. It must be noted that for splats impacting on already deposited layers, the liquid drop–substrate wettability is good (a liquid wets well a solid of the same material), and in most cases the next layers of splats impact on layers hotter than the substrate, especially if the sprayed material has a poor thermal conductivity as most oxides.

With the D-gun or high-power HVOF guns, particles must be at least in a plastic state at impact. This is particularly true for ceramic materials usually characterized by low densities and high melting points. The limitation in this case is not the

particle velocity, generally high, but the degree of melting or the plasticity. For example, for D-gun spraying, the presence of unmolten ceramic particles produces an erosive blasting effect both on the substrate and on the coating [49]. For particles in a plastic or molten state the impact of the new incoming particles results in an impact consolidation and densification of previously deposited layers (similar to shot peening effect).

Another type of adhesion is obtained when diffusion occurs between substrate and sprayed material. However, according to Eq. (2.4), this occurs only at high-substrate temperatures (about 0.6–0.7 T_m where T_m is the melting temperature), and *if the oxide layer at the substrate surface has almost disappeared*. Thus such adhesion is observed when spraying in soft vacuum a super alloy onto a super alloy substrate, and after destroying the oxide layer at the substrate surface with a reversed arc (substrate as cathode see Chap. 7).

Finally, chemical bonding can occur if the impacting droplet melts the surface and if both materials can make a new material. For that to occur, the particle effusivity e_p has to be larger than that of the substrate. The effusivity is defined as

$$e_p = \sqrt{\rho_p \cdot \kappa_p \cdot c_p} \tag{2.6}$$

where ρ_p, κ_p, and c_p are, respectively, the particle specific mass (kg/m^3), thermal conductivity (W/m s), and specific heat (J/kg K). This is the case, for example, if Mo particles are sprayed onto an iron substrate, liquid Mo can react with liquid Fe to form $MoFe_2$. For more details about particle adhesion in conventional spraying, see Sects. 13.5 and 13.6, and for submicrometric or nanometric ones, see Sect. 14.7.6.1.

2.8.2.2 Cold Particles

In the case of cold spray, the resulting splats are quite different because the deformation at impact is much less than that obtained with particles in a semimolten or molten state. Even if the adhesion process is not yet completely understood, authors agree that the high kinetic energy of particles impacting on the substrate results in cleaning and activation of the surface during what is called an induction time, generating favorable conditions for adhesion for the subsequently impacting particles [50]. As already mentioned, adhesion of the first particles to the substrate leads to a rapid increase in the number of particles attached to the substrate and consequently to the formation of a continuous coating. It seems that the plastic deformation at impact results in the rupture of superficial films, such as the oxide layer, and allows achieving an excellent contact between both pure metals at high pressure forming a metallurgical bond. Moreover, the impact of the next particle results in an impact densification of the previously deposited layers. The improvement of the contact quality increases with the impact velocity [51]. The critical velocity depends on the spray particle material and size distribution as well as the substrate material composition, roughness, hardness, and elastic modulus. For more details see Sects. 6.2.2 and 6.2.3.

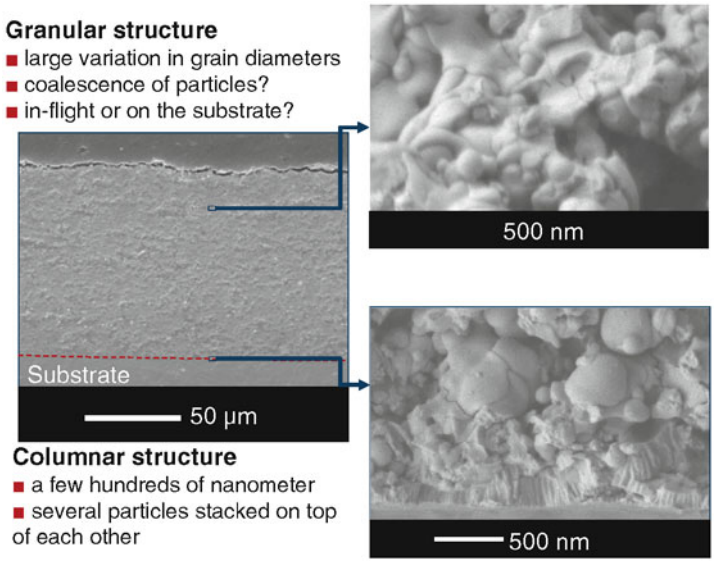

Fig. 2.30 Fractured cross section of YSZ suspension plasma sprayed (Ar–He 40–20 slm, 12 MJ/kg) onto a stainless steel substrate and detached from its substrate. Reprinted with kind permission from Springer Science Business Media [52], copyright © ASM International

2.8.3 Coatings Resulting from Solution or Suspension Spraying

At the present development stage, essentially oxide coatings or WC–Co coatings are deposited with solution or suspension spraying. For suspensions, solid particles contained in droplets, which have traveled in the hot jet core, are melted, will form splats on smooth substrates [17]. The splat diameters are at the maximum two times the initial particle diameters. Surprisingly, the corresponding coatings have a lamellar structure close to the substrate and a granular one above a few µm from the substrate as shown in Fig. 2.30.

This appearance is probably due to the very high heat flux imposed by the plasma jet at the spray distance of 3 cm (up to 40 MW/m^2) together with the Weber number of particles below 500. As the splat solidification is delayed by this strong heating, as soon as a sufficiently thick layer of zirconia has been deposited, the surface tension force takes over and the recoil phenomenon takes place. Therefore, such coatings are dense with pore sizes in the nanometer to the few hundreds of nanometers range and possess a granular structure completely different from the lamellar one obtained with conventional spraying, as illustrated in Fig. 2.32. Coatings deposited with this technology have thicknesses ranging from 5 µm to hundreds of micrometers, thus bridging the gap between coatings obtained through gaseous phase and thermally sprayed coatings.

For solutions, Gell et al. [53] have described the different mechanisms that included precursor solute precipitation, pyrolysis, sintering, melting, and crystallization. The droplet treatment by the plasma jet differs with their sizes: the larger particles correspond to the condensation of the precursor precipitating in the droplet periphery and the production of hollow spheres. Smaller droplets result in a uniform precipitation. Upon impact on the substrate, fully melted particles will produce splats as with suspensions and then, depending on spray conditions a granular structure, as with suspensions. If the standoff distance increases molten particles may resolidify and crystallize before impact. For droplets traveling in the low-temperature regions of the jet, some precursor solution can reach the substrate in liquid form (for more details see Sect. 14.7.6).

When most of the solution drops penetrate into the plasma core, mostly small droplets are obtained resulting in well-melted particles. Coatings are then dense as that shown in Fig. 2.30 suspension plasma sprayed. When drops are fragmented in the jet fringes, unpyrolized droplets are imbedded in the coating during its formation. Upon reheating by the plasma jet during the successive passes, these materials are pyrolized, sintered, and the resulting volume shrinkage promotes the formation of vertical cracks if the quantity of unpyrolized material is sufficiently high.

2.8.4 Residual Stresses

Stresses encountered during the spray process are [54]:

- *The quenching stress* (always tensile) due to cooling of each individual splat is increasing with the quality of the contact between the splat and the substrate or the splat and the previously deposited layer. This contact is improved by substrate preheating above the transition temperature.
- *The compressive stress* is due to particles impacting at high velocity (HVOF, D-gun, cold spray) equivalent to shot peening, and it can be affected by the coating temperature. These are often more important than the quenching stresses.
- *The temperature-gradient stress* develops especially within low-thermal conductivity coatings. This stress must be avoided and suppressing or reducing drastically the temperature gradients within the coating during its formation can achieve that.
- *The phase change stress* occurs when the crystal in a new phase after deposition is smaller or larger than in the preceding phase. This is for example the case when sprayed coatings essentially composed of γ alumina transform into α alumina at about 950 °C. This situation is generally encountered during service conditions, but it can also occur if too high temperature gradients are encountered during spraying of low-thermal conductivity materials. Such transformations must be avoided because ceramic coatings are generally destroyed when this transformation occurs.
- *The expansion mismatch stress* occurs during substrate and coating cooling from the mean temperature they had during spraying (deposition temperature) to room

temperature. This stress increases with the mean deposition temperature and the mismatch between the expansion coefficients of coating and substrate. Here also, for low-thermal conductivity coatings, a too fast cooling can induce damaging temperature gradients.

Of course, the final stress distribution within coating and substrate is the addition of all the previously described stresses, plus that created in the substrate by its preparation such as grit blasting. Service conditions will bring new stress, generally due to temperature gradients developed between coating surface and substrate interface either during heating or cooling phases. This stress will be added to the residual one and can result in coating detachment. The control of these different stresses, depends strongly on coating and substrate temperature during spraying, and is of primary importance for coating service conditions. With a too high residual stress, coatings can peel off, especially thick ones [54]. The level of stress-induced peeling-off depends on the coating toughness, which is drastically improved for nanostructured coatings.

2.9 Control of Coating Formation

2.9.1 Coating Temperature Control Before, During, and After Spraying

The temperature control of the substrate and coating before (preheating), during (spraying) and after spraying (cooling down) is of primary importance. Heating has to be controlled:

- During preheating with a temperature high enough to desorb adsorbates and condensates (substrate surface cleaning just before spraying during the preheating stage), but with the substrate oxidation limited as much as possible.
- At the beginning of spraying and during spraying of successive passes to limit the substrate oxidation.
- During spraying to control residual stresses formed during coating formation and then, when spraying is terminated, those due to the cooling of coating and substrate.

To limit as much as possible on the one hand the oxidation phenomena and on the other to control the stress distribution, it is necessary to control the preheating and deposition temperatures and keep them as constant as possible, especially within coating under construction when the sprayed material has a poor thermal conductivity. These temperatures depend on:

The heat flux from the hot gases during the preheating and spraying stages
The heat flux from the molten, or semimolten, droplets as they impact and stick to the substrate surface, during the spraying stage

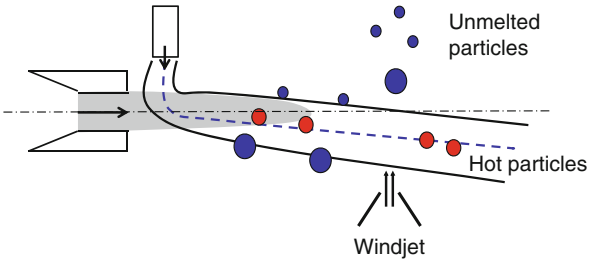

Fig. 2.31 Illustration of cold particles elimination by a windjet

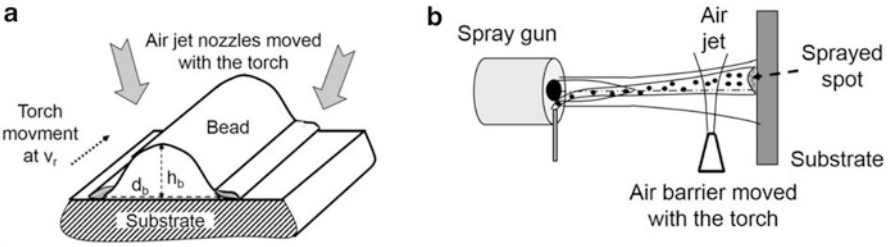

Fig. 2.32 Debris: (**a**) elimination by air jets and (**b**) reduction by an air barrier

The cooling systems used (during spraying and cooling stages). Two types of cooling systems are used with air as cooling medium: air nozzles fixed or moving with the torch and blowing onto the substrate and coating under construction, and/or wind jets moved with the torch and blowing orthogonally to the hot gases jet. Besides the reduction of the heat flux of the hot gases (up to a factor of 5), the wind jet allows eliminating those particles traveling in the fringes of the hot gas jet (see Fig. 2.31). Such particles, which generally are not melted, create defects in the coating when sticking between successive passes. The wind jet can separate them from those traveling in the hot core of the jet because their velocities are lower than those travelling in the jet core. This is achieved of course at the expense of a decrease of the in-flight hot particle temperatures (by less than 200 K) and velocity (by less than 20 m/s). Figure 2.32a shows two air jets blowing on each side of the sprayed spot and moved with the torch. These air jets also allow eliminating debris sticking to the substrate, after one pass (Fig. 2.33). Figure 2.32b shows a single air jet blown orthogonally to the hot gas jet about 2 cm in front of the substrate. It must also be kept in mind that if the coating surface is very hot, fine particles have the tendency to stick to it and form a deposit when the torch is translated to spray the next pass (see Fig. 2.33).

The heat flux of the hot gases depends on the spray process used (for example, heat fluxes increase when using HVOF spraying instead of flame), the combustion or plasma-forming gases, the spray distance (for example, with d.c. plasma jets the heat flux diminishes exponentially with the distance from the nozzle), and the relative movement torch–substrate (spray pattern) that can have a very important effect. The heat content of the sprayed particles increases with their quantity

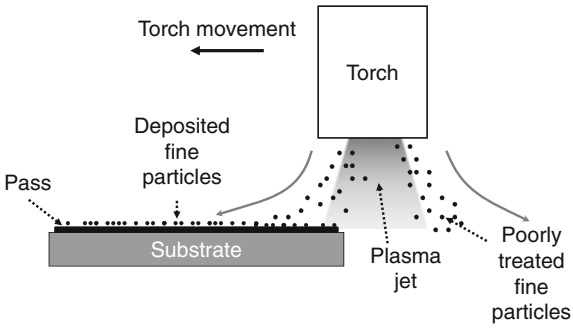

Fig. 2.33 Fine particles sticking on a hot pass

deposited during each pass. However, whatever may be the cooling system used (even cryogenic ones), most of the heat is withdrawn through conduction through the substrate. When depositing high-thermal conductivity materials (copper, for example) thick deposits can be achieved without generating steep temperature gradients. But this is not the case when spraying low-thermal conductivity materials (below 20–30 W/m K) for which thin layers (a few μm) must be deposited. For details about substrate and coating heating during the spray process see Sect. 13.8.

With plasma spraying, the mean deposition temperature is easily maintained around 400 °C during deposition, thanks to the thin passes when spraying low-thermal conductivity materials and the cooling air slot.

For stronger cooling (but also more expensive), cryogenic cooling can be used either with CO_2 snow or atomized liquid argon.

2.9.2 Control of Other Spray Parameters

Besides being influenced by the substrate temperature, any coating depends strongly on the control of the other following variables:

- The surface preparation
- The standoff distance
- The angle of impingement
- The relative velocity between the spray gun and the part to be coated
- The spray pattern

2.9.2.1 Surface Preparation

It is mandatory to clean, roughen, and clean again (to get rid of grit-blasting residues) the substrate prior to spraying. Otherwise coatings will not at all adhere to the substrate. For more details see Chap. 12 devoted to surface preparation (see Sect. 12.3).

2.9.2.2 Standoff Distance

This distance, also called spray distance, i.e., the distance between the nozzle exit and the part to be coated, is a compromise. It should be the distance where the average sized particle has reached the maximum temperature and velocity because farther downstream both these quantities diminish. However, at this distance (except for cold spray), in most cases the heat flux of the hot jet is still very high, especially for plasma spraying. For example, in plasma spraying with an Ar–H_2 jet, the optimum distance for particles is in the 50–60 mm range. However the heat flux values are in the range 4–8 MW/m^2. Thus spray distances are chosen between 90 and 120 mm in order to have heat fluxes below 2 MW/m^2.

2.9.2.3 Impact Angle

Studies have been devoted to this topic [55]. Splats collected on inclined surfaces present the same adhesion as those sprayed with an impact angle of 90° as long as the angle is between 60 and 90°. Depending on substrate and sprayed material, the adhesion is acceptable down to 45° and decreases drastically after that. Thus it is recommended to spray with an impact angle as close as possible to 90°. For more details see Sect. 13.5.2.

2.9.2.4 Beads

A bead is obtained when translating the torch relative to the substrate at a given relative velocity v_r. The bead height h_b and width d_b at mid-height depend on v_r, the powder mass flow rate, deposition efficiency, torch nozzle internal diameter, and injection conditions. In most cases the bead shape is Gaussian in good agreement with the distribution of hot particles. In the wings of the bead (see Fig. 2.32a), frequently particles appear which are not well exposed to the hot jet, but are sufficiently heated to stick. These particles, at least the metallic ones, are easily oxidized and they may form the major source of oxide inclusions in sprayed coatings, and thus create defects. Another important point is the risk, when spraying off-normal angles [55], to have particles intercepted by the bead rebounding and splashing on the other side of it. The adhesion of the splashed material being very poor, it will be the same with the next bead deposited on top of it [56]. For more details see Sect. 13.7.1.3.

2.9.2.5 Passes

A pass results from the overlapping of successive beads depending on the spray pattern (see Sect. 13.7.1.4 for details). The choice of the beads overlapping ratio depends on their thickness and the surface undulation that is acceptable. For a

medium thick bead (7–8 μm) an overlap of one half-bead width results in an undulation of about 3 μm, while with an overlap ratio of 1/6, the undulation is about 1 μm [57]. The resulting pass thickness depends on the bead thickness, and the successive beads overlap. The pass thickness generally ranges between 5 and 40 μm. For materials with thermal conductivities below 20–30 W/m K, it is necessary to have thin passes (below 10 μm) to avoid too high temperature gradients in coatings. The thinner the pass, the easier is the coating and substrate cooling and thus the control of the mean temperature.

2.10 Summary and Conclusions

This section aimed at presenting globally the different thermal spray processes, the sprayed materials (powders, wire, cored wire, cord, rod), the interactions of sprayed materials, and high-energy jets produced by the different spray processes, the way coatings are constructed with the influence of the in-flight parameters and substrate preparation on coating properties and residual stresses… All these phenomena and the fundamental mechanisms involved are described in detail in the following chapters (from 3 to 18).

Nomenclature

Latin Alphabet

a Particle surface (m^2)
c_p The specific heat of the particle (J/kg K)
d_i Nozzle internal diameter (mm)
d_p Particle diameter (μm)
e_p Effusivity $e_p = \sqrt{\rho_p \cdot \kappa_p \cdot c_p}$ $\left(J/m^2\,K\,s^{0.5}\right)$
E_A Activation energy of the reaction (J)
h Gas heat transfer coefficient (W/m^2 K)
k Specific reaction rate constant
k_B Boltzmann constant (1.38×10^{-23} J/K)
L_m Latent heat of melting of the particle (J/kg)
m_p Mass of the particle (kg)
q_{cv} Heat transferred to a particle by the hot gas (W)
Q_F Energy necessary to melt the particle (J)
Q_L Define the requirement for melting a particle ($J\,m^{3/2}/kg^{0.5}$)
v_g Gas velocity (m/s)
v_p Particle velocity (m/s)
T_s Gas temperature (K)

Greek Alphabet

ε Global emission coefficient of the particle
μ_g Gas viscosity (xx)
κ Thermal conductivity (W/m K)
ρ_p Particle specific mass (kg/m^3)
σ_S Stefan–Boltzmann radiation constant (5.671×10^{-8} W/m^2 K^4)
τ Residence time of the particle in the hot jet (s)

References

1. Cartier M (2003) Handbook of surface treatments and coatings. ASME Press, New York, NY
2. Davis JR (ed) (2004) Handbook of thermal spray technology. ASM International, Materials Park, OH
3. Chattopadhyay R (2001) Surface wear. ASM International, Materials Park, OH
4. Kanani N (2004) Electroplating, basic principles, processes and practice. Elsevier, Amsterdam
5. Djokic SS (2010) Electroless deposition: theory and applications, chapter 6. In: Djokic SS, Cavallotti P (eds) Modern aspects of electrochemistry, vol 48. Springer, New York, NY, pp 251–289
6. Maaß P, Peißker P (2011) Handbook of hot-dip galvanization. Wiley, New York, NY, 494 p
7. Dobkin DM, Zuraw MK (2003) Principles of chemical vapor deposition. Kluwer Academic, Dordrecht
8. Pawlowski L (2003) Dépôts physiques. Presses polytechniques et universitaires romandes, Lausanne
9. Glocker DA, Shah SI (1995) Handbook of thin film process technology (2 vol. set). Institute of Physics, Bristol
10. Mahan JE (2000) Physical vapor deposition of thin films. Wiley, New York, NY
11. Erkens G, Vetter J, Müller J, auf dem Brinke T, Fromme M, Mohnfeld A (2011) Plasma-assisted surface coating processes, methods, systems and applications. Sulzer Metco, Süddeutscher Verlag onpact GmbH, Munich
12. Frey H, Khan HR (2013) Handbook of thin film technology. Springer, Berlin, 550 pages
13. Gladush GG, Smurov I (2011) Physics of laser materials processing: theory and experiment, Springer series in materials science. Springer, Berlin
14. American Welding Society (1985) Thermal spraying, practice, theory and application. American Welding Society, Miami, FL
15. Pawlowski L. The science and engineering of thermal spray coatings. Wiley, New York, NY, 1st edition (1995) and 2nd edition (2008)
16. Seyed A. Co-spraying of alumina and stainless steel by d.c. plasma jets. PhD Thesis, University of Limoges France and GIK Institute, Topi, Pakistan, 26 Feb 2004, Limoges France
17. Fauchais P, Etchart-Salas R, Rat V, Coudert J-F, Caron N, Wittmann-Ténèze K (2008) Parameters controlling liquid plasma spraying: solutions, sols or suspensions. J Therm Spray Technol 17(1):31–59
18. Scrivani A, Bardi U, Carrafiello L, Lavacchi A, Niccolai F, Rizzi G (2003) A comparative study of high velocity oxygen fuel, vacuum plasma spray, and axial plasma spray for the deposition of CoNiCrAlY bond coat alloy. J Therm Spray Technol 12(4):504–507
19. Yankee SJ, Salsbury RL, Pletka BJ (1991) Quality control of hydroxylapatite coating: properties, processes and applications. In: Bernecki T (ed) Thermal spray 1991. ASM International, Materials Park, OH, pp 475–483

20. Fauchais P, Fukumoto M, Vardelle A, Vardelle M (2004) Knowledge concerning splat formation: an invited review. J Therm Spray Technol 13(3):337–360
21. Gärtner F, Stoltenhoff T, Schmidt T, Kreye H (2006) The cold spray process and its potential for industrial applications. J Therm Spray Technol 15(2):223–232
22. Champagne VK (ed) (2007) The cold spray materials deposition process. Woodhead Publishing Limited, England
23. Alkhimov AP, Papyrin AN, Kosarev VF, Nesterovich NI, Shushpanov MM. Gas-dynamic spraying method of applying a coating. US Patent 5, 302,414, April 12.
24. Stoltenhoff T, Kreye H, Richter HJ (1994) An analysis of the cold spray process and its coatings. J Therm Spray Technol 11(4):542–550
25. Kashirin AI, Klynev OF, Buzdygar TV (2002) Apparatus dynamic coating. US patent 6, 402, 050, June 11
26. Shkodkin A, Kashirin A, Klynev O, Buzdygar T (2006) Metal particle deposition simulation by surface abrasive treatment in gas dynamic spraying. J Therm Spray Technol 15(3):382–386
27. Kashirin A, Klynev O, Buzdygar T, Shkodin A (2007) DYMET technology evolution and application. In: Marple BR et al (eds) Thermal spray 2007: global coating solutions. ASM International, Materials Park, OH, e-proceedings
28. Hermanek FJ (2001) Thermal spray terminology and company origins. ASM International, Materials Park, OH
29. Glassmann I (1977) Combustion. Academic, New York, NY
30. Ducos M (2006) Evaluation des coûts de projection thermique (Costs evaluation in thermal spraying). Cours, ALIDERTE, Limoges
31. Thorpe ML, Richter HJ (1992) A pragmatic analysis and comparison of HVOF processes. J Therm Spray Technol 1(2):161–170
32. Smith MF, Dykhuisen RC, Neiser RA (1997) Oxidation in HVOF sprayed steels. In: Berndt CC (ed) Thermal spray: a united forum for scientific and technological advances. ASM International, Materials Park, OH, pp 885–892
33. Kadyrov E, Kadyrov V (1995) Gas dynamical parameters of detonation powder spraying. J Therm Spray Technol 4(3):280–286
34. Fauchais P (2004) Understanding plasma spraying, an invited review. J Phys D Appl Phys 37:2232–2246
35. Morishita T (1991) In: Blum–Sandmeier S et al. Plasma Technik 2nd symposium, vol. 1. Plasma Technik, Wohlen, pp 137–145
36. Boulos M (1992) RF induction plasma spraying: state-of-the-art review. J Therm Spray Technol 1:33–40
37. Bolot R, Planche M-P, Liao H, Coddet C (2008) A three-dimensional model of the wire-arc spray process and its experimental validation. J Mater Process Technol 200:94–105
38. Wilden J, Bergmann JP, Frank H (2006) Plasma transferred arc welding-modeling and experimental optimization. J Therm Spray Technol 15(4):779–784
39. Vardelle M, Vardelle A, Fauchais P, Li K-I, Dussoubs B, Themelis NJ (2001) Controlling particle injection in plasma spraying. J Therm Spray Technol 10:267–286
40. Dolatabadi A, Pershin V, Mostaghimi J (2005) New attachment for controlling gas flow in the HVOF process. J Therm Spray Technol 14(1):91–99
41. Hussary NA, Heberlein JVR (2001) Atomization and particle jet interactions in the wire-arc spraying process. J Therm Spray Technol 10(4):604–610
42. Filkova I, Cedik P (1984) Nozzle atomization in spray drying, vol 3. In: Mujumdar AS (ed) Advances drying. Hemisphere Publishing Corporation, pp 181–215
43. Savkar FD, Siemers PA (1989) Some recent developments in rapid solidification plasma deposition technology. In: Boulos M (ed) Workshop applications, pp 80–89
44. Neiser RA, Smith MF, Dykhuisen RC (1998) Oxidation in wire HVOF-sprayed steel. J Therm Spray Technol 7(4):537–545
45. Pasandideh-Fard M, Pershin V, Chandra S, Mostaghimi J (2002) Splat shapes in a thermal spray coating process: simulations and experiments. J Therm Spray Technol 11(2):206–217

46. Fukumoto M, Haang Y (1999) Flattening mechanism in thermal sprayed Ni particles impinging on flat substrate. J Therm Spray Technol 8(2):427–432
47. Chandra S, Fauchais P (2009) Formation of solid splats during thermal spray deposition. J Therm Spray Technol 18(2):148–180
48. Klinkov SV, Kosarev VF (2006) Measurements of cold spray deposition efficiency. J Therm Spray Technol 15(3):364–371
49. Kadyrov V (1992) Detonation coating technology. J Jpn Therm Spray Soc 29(4):14–25
50. Raletz F, Vardelle M, Ezoo G (2006) Critical particle velocity under cold spray conditions. Surf Coat Technol 201(5):1942–1947
51. Papyrin AN, Klinkov SV, Kosarev VF (2005) Effect of the substrate surface activation on the process of cold spray coating formation. In: Lugscheider E (ed) Thermal spray 2005. DVS, Dusseldorf, Germany, e-proceedings
52. Bacciochini A (2010) Quantification of porous architecture of finely structured deposits of yttria stabilized zirconia manufactured by suspension plasma spraying. PhD Thesis, University of Limoges, France, 24 Nov
53. Gell M, Jordan E, Teicholz M, Cetegem BM, Padture NP, Xie L, Chen D, Ma X, Roth J (2008) Thermal barrier coatings made by the solution precursor plasma spray process. J Therm Spray Technol 17(1):124–135
54. Clyne TW, Gill SC (1996) Residual stresses in thermal spray coatings and their effect on interfacial adhesion: a review of recent work. J Therm Spray Technol 5(4):401–418
55. Smith MF, Neiser RA, Dykhuizen RL (1994) An investigation of the effects of droplet impact angle in thermal spray deposition. In: Berndt CC, Sampath S (eds) Thermal spray: industrial applications. ASM International, Materials Park, OH, pp 603–608
56. Kanaouff MP, Neiser RA, Roemer TJ (1998) Surface roughness of thermal spray coatings made with off-normal spray angle. J Therm Spray Technol 7(2):219–231
57. Montillet D, Dombre E, Valentin FD, Goubot JM (1999) Modeling, simulating and optimizing the robotized plasma deposition: an expression approach. In: Lugsheider E, Kammer PA (eds) Thermal spray. DVS, Düsseldorf, Germany, pp 507–512

http://www.springer.com/978-0-387-28319-7

Thermal Spray Fundamentals
From Powder to Part
Fauchais, P.L.; Heberlein, J.V.R.; Boulos, M.I.
2014, LVI, 1566 p. 953 illus., 235 illus. in color. In 2 volumes, not available separately., Hardcover
ISBN: 978-0-387-28319-7